1970

Unsymmetrical plate girders. Under shear and moment, October 1970

Chingmiin Chern

Alexis Ostapenko

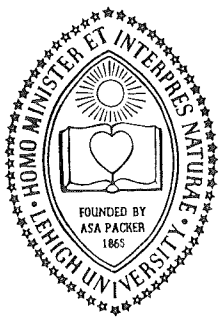

LEHIGH UNIVERSITY

OFFICE
OF
RESEARCH

UNSYMMETRICAL PLATE GIRDERS UNDER SHEAR AND MOMENT

by
Chingmiin Chern
and
Alexis Ostapenko

October 1970

Fritz Engineering Laboratory Report No. 328.9C

UNSYMMETRICAL PLATE GIRDERS UNDER SHEAR AND MOMENT

by

Chingmiin Chern

and

Alexis Ostapenko

This work was conducted as part of the project Unsymmetrical Plate Girders, sponsored by the American Iron and Steel Institute, the Pennsylvania Department of Transportation, the Federal Highway Administration of the U.S. Department of Transportation, and the Welding Research Council. The findings and conclusions expressed in this report are those of the authors, and not necessarily those of the sponsors.

Department of Civil Engineering
Fritz Engineering Laboratory
Lehigh University
Bethlehem, Pennsylvania

October 1970

Fritz Engineering Laboratory Report No. 328.9

TABLE OF CONTENTS

UNSYMMETRICAL PLATE GIRDERS UNDER SHEAR AND MOMENT

by

Chingmiin Chern[1]

and

Alexis Ostapenko[2]

ABSTRACT

A method of determining the ultimate static strength of transversely stiffened plate girders subjected to a combination of shear and bending is presented. The method is applicable to homogeneous and hybrid girders with symmetrical or unsymmetrical cross section. The ultimate strength is assumed to be given by the sum of three contributions: beam action, tension field action and frame action. In the web plate buckling computation, the web is assumed to be fixed at the flanges and simply supported at the stiffeners. The behavior of a girder panel is described by a continuous interaction curve which is divided into three parts: web failure portion, compression flange buckling portion and tension flange yield portion. The theoretical ultimate loads compare well with the results of the available fifty-three tests on symmetrical and unsymmetrical plate girders. The average deviation is 5% with the extreme deviation of 15%.

[1]Assistant Professor of Civil Engineering, North Dakota State University, Fargo, N.D., formerly Research Assistant at Lehigh University, Bethlehem, Pennsylvania

[2]Professor of Civil Engineering, Fritz Engineering Laboratory, Department of Civil Engineering, Lehigh University, Bethlehem, Pennsylvania

1. INTRODUCTION

A plate girder in a building or in a bridge has a majority of its panels subjected to some combination of shear and moment; only a few panels would ordinarily be under pure moment or shear. Yet, most of the theoretical and experimental research conducted so far on the ultimate strength of plate girders has dealt with the simpler cases of pure moment or shear, and the case of combined loads* has been treated due to its complexity as some plausible transition between these two strengths.

In 1961, Basler suggested that the moment capacity of a plate girder section be given by the yield strength of the flanges plus the yield capacity of the web reduced by a shear stress assumed to be uniform. The effect of web buckling was neglected and the approach is thus valid only for webs with very low depth-thickness ratios. To overcome this difficulty it was proposed that the shear capacity V_u (including the post-buckling strength) be not reduced by bending up to $M = 0.75$ of the pure bending moment M_y, causing yielding of the tension flange, and the moment capacity M_y be not reduced by shear up to $V = 0.60$ of the pure shear strength V_u. The transition between the two resulting points was assumed to be a straight line. If applicable, the moment from this interaction diagram should be reduced to M_u which is primarily controlled by the strength of the compression flange.(4) This interaction relationship was then adopted by the AISC

---

*Hereafter, whenever there is no possibility of confusion, "combination of moment and shear" will be called "combined loads."

Specification.[2] Reference 24 introduced a modification of the method by replacing the tension flange yield moment M_y with the ultimate moment for pure bending M_u.

In 1968, Akita and Fujii arrived at another interaction relationship consisting of three straight lines.[1] The end points were assumed to be given by the ultimate strengths for pure shear V_u and pure moment M_u. One of the intermediate two points was defined by the shear causing pure shear buckling of the web and by the moment produced by the yielded flanges. The other point was given by the ultimate shear of the web computed assuming the flanges to be of zero rigidity, and the moment produced by the flanges yielded under the axial forces due to bending and the tension field action. The method neglects the possibility that the compression flange may buckle laterally.

In all the above described studies, only girder panels with symmetrical cross sections were considered. However, in many practical plate girders the cross section is unsymmetrical, that is, the centroidal axis is not at the mid-depth of the web; most typically, this is the case for composite and orthotropic deck girders. So far, the only consideration given to unsymmetrical girders is an adaptation of Basler's interaction relationship[4] in Reference 24.

The purpose of the present study is to describe a new method which gives the ultimate strength of a plate girder panel directly for any combination of moment and shear and is applicable to unsymmetrical, symmetrical, homogeneous, and hybrid girders. The analytical model of the method and the assumed pattern of the girder behavior are given next.

Due to the complexity of the force interaction in a plate girder panel, an exact analysis of its behavior under load has been impossible, and recourse had to be taken to represent the panel in the form of a model as closely to the true state as possible and formulating the desired strength equations on it. Deficiencies of the analytical models employed by previous researchers have been pointed out. The model proposed here, although not perfect, provides a means for explaining cases which could not be handled before.

The model for combined loads represents an interaction between the models which have been developed in the course of this research for the cases of pure shear[7] and pure bending.[8] The web plate is assumed to be flat until it buckles under the combined effect of increasing stresses due to shear and moment. The post-buckling strength of the web is assumed to be in the form of the tension field action analogous to, but not the same as, in References 1 and 3. The contribution of it is limited by the yielding of the web plate and both, shear and moment, are taken into account.

The flanges together with an effective area of the web contribute to the shear strength by forming a plastic mechanism with hinges at the stiffeners (Frame Action). The effect of the axial forces in the flanges is included. The axial strength of the flanges in yielding or buckling (lateral or torsional) controls the magnitude of the moment on the panel. The horizontal component of the tension field force reduces the flange capacity available to carry the moment. When the flange buckling capacity is reached before the full capacity of the web or frame action is developed, the reduction of the moment due to their presence is proportionately smaller.

The modes of behavior described above are equally valid whether the larger portion of the web is in tension or compression, except that a full plastification of the web may be possible as the web portion under compression becomes smaller. Depending on whether or not the flanges fail before the shear capacity of the panel is developed, two types of interaction between shear and moment are possible; shear capacity reduced by moment, and moment capacity reduced by shear. One or the other will control the design. A complete interaction relationship is thus established.

Since for a given pattern of loading, both shear and moment are directly proportional to the intensity of loads, it is convenient to visualize any panel as if it were a panel in a simply supported beam under a mid-span concentrated load as shown in Fig. 1. Then the maximum moment in the panel is $M_{max} = Vx$ and the mid-panel moment is $M = V(x - \frac{1}{2}a)$ for any intensity of loading. This idealization is employed later in the derivation of the strength equations.

2. ANALYTICAL MODEL AND INTERNAL FORCES

The static ultimate strength of a girder panel under combined shear and bending expressed by means of shear force is assumed to be given by a sum of the following three contributions: (a) the beam action shear $V_{\tau c}$; (b) the tension field action shear $V_{\sigma c}$; and (c) the frame action shear V_{fc}.

$$V_{th} = V_{\tau c} + V_{\sigma c} + V_{fc} \tag{1}$$

Each of the shears in Eq.1 is computed considering the effect of the bending moment.*

Beam Action Strength. - Figure 2 shows a rectangular web plate subjected to combined loads. The top fiber compression stress is positive, and shear is positive when it acts down on the right hand face. The web stresses at the buckling load may be evaluated with sufficient accuracy by means of the following interaction equation: (15)

$$\left(\frac{\tau_c}{\tau_{cr}}\right)^2 + \frac{1+C}{2}\left(\frac{\sigma_{bc}}{\sigma_{cp}}\right) + \frac{1-C}{2}\left(\frac{\sigma_{bc}}{\sigma_{cp}}\right)^2 = 1.0 \tag{2}$$

---

* The effect of the moment is not considered for the pure shear case described in Reference 7. Subscript "c" in Eq.1 and subsequent equations designates "combined" to differentiate from analogous notation in References 7 and 8.

where

τ_c = shear stress at buckling under combined loads

$\tau_{cr} = k_v \frac{\pi^2 E}{12(1-\nu^2)}\left(\frac{t}{b}\right)^2$, buckling stress under pure shear

with the shear buckling coefficient

$$k_v = \frac{5.34}{\alpha^2} + \frac{6.55}{\alpha} - 13.71 + 14.10\,\alpha \qquad (3a)$$

for $\alpha \leq 1.0$

or

$$k_v = 8.98 + \frac{6.18}{\alpha^2} - \frac{2.88}{\alpha^3} \qquad (3b)$$

for $\alpha \geq 1.0$

α = a/b, panel aspect ratio, or the ratio of the panel length to panel depth

σ_{bc} = bending stress at the extreme compression fiber of the web when the plate buckles under combined loads

$\sigma_{cp} = k_b \frac{\pi^2 E}{12(1-\nu^2)}\left(\frac{t}{b}\right)^2$, stress at the extreme compression fiber of the web buckling under pure bending

with the bending buckling coefficient k_b taken at its minimum value neglecting the effect of α (or setting $\alpha = \infty$)

$$k_b = 13.54 - 15.64\,C + 13.32\,C^2 + 3.38\,C^3 \qquad (4)$$

for $-1.5 \leq C \leq 0.5$

C = ratio of maximum tensile stress to maximum compressive stress for the combined loading case as shown in Fig.2.

Then, the shear force carried by the web at the web buckling load is

$$V_{\tau c} = \tau_c A_w = \tau_c\, bt \qquad (5)$$

As a simplification of further analysis it is assumed that the stress is constant over the flange thickness and is equal to the stress at the web boundaries. Then, at the web buckling load the stress in the compression flange is

$$\sigma_{1c} = \sigma_{bc} \tag{6a}$$

and the magnitude of the stress in the tension flange is

$$\sigma_{1t} = -C \ \sigma_{bc} \tag{6b}$$

Tension Field Action Strength. - In evaluating the ultimate strength of the web, three additional assumptions are made: (a) the web stresses remain constant after the plate buckles, (b) the linearly varying compressive and tensile stresses may be replaced by their average values (this assumption introduces only a negligible inconsistency between the total external and internal moments), and (c) the ultimate strength is attained when the combination of the shear buckling stress under combined loads, the average tensile stresses and the tension field stress reaches the yield condition. The idealized tension field model under combined loads is shown in Fig.3 where angle ϕ_c indicates the inclination of the tension field.

The process of deriving the equation for the tension field action shear $V_{\sigma c}$ starts by transforming the state of stress defined by τ_c and σ_{bc} to the coordinate axes forming the yet unknown angle ϕ_c with the horizontal direction (see Fig. 3).

The normal stress in the direction of ϕ_c is then increased by σ_{tc} and the von Mises yield condition is imposed on the resulting combined state of stress. After some manipulations a relationship is obtained as given by Eq. 7 in which σ_{tc} and ϕ_c are the unknowns.

$$\sigma_{tc} = \sigma_{yw}\sqrt{\left[1-3\left(\frac{R}{\sigma_{yw}}\right)^2-\left(\frac{S}{2\sigma_{yw}}\right)^2\right]+\left[\frac{1}{2}\left(\frac{S}{2\sigma_{yw}}\right)+\frac{3}{2}\left(\frac{R}{\sigma_{yw}}\right)\ \text{Sin}\ (2\phi_c+2\delta)\right]^2}$$

$$-\left[\frac{1}{2}\left(\frac{S}{2}\right)+\frac{3}{2}\,R\ \text{Sin}\ (2\phi_c+2\delta)\right] \qquad (7)$$

where

$$S = -\frac{C}{2}\left[\sigma_{bc}\right]$$

$$R = \sqrt{\left(\frac{S}{2}\right)^2+\tau_c{}^2}$$

$$\delta = \frac{1}{2}\ \tan^{-1}\left(\frac{S}{2\tau_c}\right)$$

The moment at the mid-panel section is defined as shown in Fig. 1 and on page 5 in terms of the longitudinal distance from the point of zero moment to the far end of the panel under investigation. For the convenience of further discussion, this moment from now on will be defined in terms of the shear span ratio μ.

$$\mu = \frac{M}{bV} = \frac{x - a/2}{b} \qquad (8)$$

The tension field shear is found from the stress diagram in Fig.4b to be

$$V_{\sigma c} = \frac{1}{2} A_w \sigma_{tc} \left[\text{Sin } 2\phi_c - (1 - \rho)\ \alpha + (1 - \rho)\ \alpha \text{ Cos } 2\ \phi_c \right] \qquad (9)$$

As shown in Reference 7, a conservative estimate of the parameter ρ for a plate girder is

$$\rho = 0.5 \qquad (10)$$

Now, with parameter ρ being constant and the panel having the given geometrical and material properties, σ_{tc} is a function of ϕ_c only. Equation 9 thus can be rewritten as

$$V_{\sigma c} = V_{\sigma c}\ (\phi_c)$$

in which ϕ_c is the only variable. The maximum value of $V_{\sigma c}$ is obtained by setting the derivative of the function with respect to ϕ_c equal to zero,

$$\frac{\partial V_{\sigma c}}{\partial \phi_c} = 0$$

This gives the following expression for ϕ_{co}, the value of ϕ_c for which $V_{\sigma c}$ is a maximum:

$$[\text{Sin } 2\phi_{co} - (1-\rho)\alpha + (1-\rho)\,\alpha \text{ Cos } 2\phi_{co}] \frac{\partial \sigma_{tc}}{\partial \phi_{co}}$$

$$+ 2\,[\text{Cos } 2\phi_{co} - (1-\rho)\,\alpha \text{ Sin } 2\phi_{co}]\,\sigma_{tc} = 0 \qquad (11)$$

Equation 11 can be solved for ϕ_{co} by iteration. (An iteration method is explained in the Appendix of Ref.7). Substituting ϕ_{co} back into Eqs. 7 and 9 gives the maximum tension field contribution becomes

$$V_{\sigma c} = \frac{1}{2} A_w \sigma_{tc} \; [\text{Sin } 2\,\phi_{co} - (1-\rho)\,\alpha + (1-\rho)\,\alpha \text{ Cos } 2\,\phi_{co}] \qquad (12)$$

where

$$\sigma_{tc} = \sigma_{yw}\sqrt{\left[1 - 3\left(\frac{R}{\sigma_{yw}}\right)^2 - \left(\frac{S}{2\,\sigma_{yw}}\right)^2\right] + \left[\frac{1}{2}\left(\frac{S}{2\,\sigma_{yw}}\right) + \frac{3}{2}\left(\frac{R}{\sigma_{yw}}\right) \text{Sin } (2\phi_{co} + 2\delta)\right]^2}$$

$$- \left[\frac{1}{2}\left(\frac{S}{2}\right) + \frac{3}{2} R \text{ Sin } (2\,\phi_{co} + 2\delta)\right] \qquad (13)$$

Flange stresses under the optimum tension field shear are shown in Fig. 6b. There are two contributions: one comes from the horizontal component of the tension field force, and the other comes from the moment equilibrium for the tension field action shear. Thus, the stress in the compression flange is

$$\sigma_{2c} = \mu \frac{V_{\sigma c}}{A_{fc}} + \frac{\sigma_{tc}\, A_w}{4\, A_{fc}} [1 + \text{Cos } 2\phi_{co} - (1-\rho)\,\alpha \text{ Sin } 2\phi_{co}]$$

and the stress in the tension flange is

$$\sigma_{2t} = \mu \frac{V_{\sigma c}}{A_{ft}} - \frac{\sigma_{tc} A_w}{4 A_{ft}} [1 + \text{Cos } 2\phi_{co} - (1 - \rho) \alpha \text{ Sin } 2\phi_{co}]$$

Let

$$H = \frac{1}{2} \sigma_{tc} A_w [1 + \text{Cos } 2\phi_{co} - (1 - \rho) \alpha \text{ Sin } 2\phi_{co}] \quad (14)$$

represent the horizontal component of the tension field force which is equally carried by the top and bottom flanges.

$$\sigma_{2c} = \frac{1}{A_{fc}} [\mu V_{\sigma c} + \frac{1}{2} H] \quad (15a)$$

$$\sigma_{2t} = \frac{1}{A_{ft}} [\mu V_{\sigma c} - \frac{1}{2} H] \quad (15b)$$

Frame Action Strength. - Analogously to the frame action strength developed in Ref.7 for the case of pure shear, it is assumed for the case of combined loads that the maximum shear contribution of the flanges is reached when the plastic hinges form at both ends of the flanges to develop a panel mechanism shown in Fig.5.

$$V_{fc} = \frac{1}{a} (m_{cl} + m_{cr} + m_{tl} + m_{tr}) \quad (16)$$

where m_{cl} and m_{cr} are, respectively, the plastic moments of the compression flange at the left and right sides of the panel modified for the effect of

the axial force in the flange. m_{tl} and m_{tr} are the analogous plastic moments in the tension flange. Since the cross section of each flange is unsymmetrical, being assumed to consist of the flange proper and an effective portion of the web (see Refs. 7 and 8), the axial force influences the plastic moments at the left and right sides of the panel to a different degree and they are, therefore, not equal to each other. The compression and tension flange stresses, σ_{3c} and σ_{3t}, are produced by this action, as shown in Fig. 6c,

$$\sigma_{3c} = \mu \frac{V_{fc}}{A_{fc}} \tag{17a}$$

$$\sigma_{3t} = \mu \frac{V_{fc}}{A_{ft}} \tag{17b}$$

Reference Stresses in the Flanges. - The following flange stresses serve as reference stresses to describe the behavior of a girder panel under combined shear and bending:

(a) σ_{sc} -- the sum of the compression flange stresses contributed by the beam, tension field, and frame actions.

$$\sigma_{sc} = \sigma_{1c} + \sigma_{2c} + \sigma_{3c}$$

(b) σ_{st} -- the sum of the tension flange stresses contributed by the beam, tension field, and frame actions.

$$\sigma_{st} = \sigma_{1t} + \sigma_{2t} + \sigma_{3t}$$

(c) σ_{cf} -- the maximum stress that the compression flange can resist. It is taken to be equal to the

buckling stress of a column formed by the compression flange with a portion of the web plate. (3,7,8)

(d) σ_{yt} -- the maximum stress that the tension flange can resist. If the strain hardening is neglected, it is equal to the yield stress of the tension flange.

3. ULTIMATE STRENGTH

The failure of a panel subjected to a combination of shear and moment, may be due to the failure of the web, buckling of the compression flange or yielding of the tension flange. The occurrence of one or the other mode of failure is determined by comparing reference stresses in the flanges and selecting the lower as the controlling one. The regions for each of the three modes of failure are shown in Fig.7 where the shear is plotted against moment at the controlling ultimate condition. The non-dimensionalizing values V_u and M_u are, respectively, the ultimate shear capacity with the moment equal to zero (Ref.7) and the ultimate moment capacity with the shear equal to zero (Ref.8). As seen in the figure, the interaction curve represents a series of stress inequality relationships. The interaction curve is separated by the ordinate V/V_u into two portions: the larger portion of the web in compression and the larger portion of the web in tension, as indicated in the figure by portions Q_1 -Q_2 -Q_3 and Q_1-Q_4 -Q_5, respectively.

Larger Portion of the Web in Compression (Q_1-Q_2-Q_3). - The ultimate strength equations are formulated from the conditions in specific portions of the interaction curve.

(a) At point Q_1 in Fig. 7, the panel is under pure shear, that is, M = 0. The capacity will be limited by the web plate failure and $V_{th} = V_u$.[7]

(b) Portion between Q_1 and Q_2. The panel is under high shear and relatively low moment. When the web is stressed to its ultimate capacity under combined loads, the total stress σ_{sc} introduced to the compression flange is still less than the flange ultimate carrying capacity σ_{cf}. At this stage, the flange is strong enough to resist buckling, and the failure mechanism of the panel is the web plate failure. Therefore, the ultimate strength equations are

$$V_{th} = V_{\tau c} + V_{\sigma c} + V_{fc} \tag{18a}$$

$$M_{th} = V_{th} (x - \tfrac{1}{2} a) = \mu b V_{th} \tag{18b}$$

where $V_{\tau c}$, $V_{\sigma c}$, and V_{fc} are obtained respectively from Eqs. 5,12 and 16.

(c) At point Q_2 the stress in the compression flange due to the ultimate shear strength under combined loads is equal to the buckling stress of the compression flange column, $\sigma_{sc} = \sigma_{cf}$, and failure may occur simultaneously in the compression flange and in the web plate.

(d) Portion $Q_2 - Q_3$. If the web stress increased to the ultimate shear strength, the compressive flange stress σ_{sc} would be greater than σ_{cf}, the ultimate stress the compression flange can resist. Therefore, in this range, the web does not reach its ultimate shear strength, and the panel fails due to the buckling of the compression flange.

In order to calculate the panel strength, the following assumptions are made: the tension field model is preserved and the incomplete tension field stress is in a direct proportion to the maximum tension field stress σ_{tc}. The stresses introduced to the compression flange due to the post-buckling behavior are then

$$\sigma_{2c} + \sigma_{3c} = \sigma_{cf} - \sigma_{1c} \tag{19a}$$

$$= \sigma_{cf} - \sigma_{bc}$$

In ordinary plate girders, the shear capacity contributed by the frame action is usually less than one-tenth of the ultimate shear strength.[7] When the panel is under the combined loads, the shear capacity of the flanges will be further reduced because of the axial forces acting on the flanges. Thus, the higher is the moment on

the panel the lower is the frame action shear that can be developed. Therefore, no significant error will be introduced if σ_{3c} is assumed to be a known quantity given by Eq. 17a.* Thus, the reference flange stress due to the horizontal component of the tension field force becomes

$$\sigma_{2c} = \sigma_{cf} - \sigma_{bc} - \mu \frac{V_{fc}}{A_{fc}} \tag{19b}$$

Observing that Eqs. 15a and 19b give the same stress σ_{2c}, the following equation is obtained:

$$\mu V'_{\sigma c} + \tfrac{1}{2} H' = (\sigma_{cf} - \sigma_{bc}) A_{fc} - \mu V_{fc}$$

from which the horizontal component of the tension field force H' is found by utilizing Eqs. 13 and 14.

$$H' = \Omega V'_{\sigma c}$$

where

$$\Omega = \cot \phi_{co} \tag{19c}$$

The incomplete tension field shear $V'_{\sigma c}$ is from the above

---

*A correcting refinement can be made by varying the frame action contribution, for example linearly, from the full value of σ_{3c} at point Q_2 to zero at point Q_3.

$$V_{\sigma c}' = \frac{(\sigma_{cf} - \sigma_{bc})\, A_{fc} - \mu\, V_{fc}}{\mu + \Omega/2} \qquad (19d)$$

Then, the ultimate strength equations for $\sigma_{sc} > \sigma_{cf}$ (region Q_2- Q_3) are:

$$V_{th} = V_{\tau c} + V_{\sigma c}' + V_{fc} \qquad (19e)$$

and

$$M_{th} = V_{th}\,(x - \tfrac{1}{2}\, a) = \mu b\, V_{th} \qquad (19f)$$

(g) At point Q_3, the panel is under pure bending, that is, $V_{th} = 0$, and the failure mechanism will be due to the failure of the compression flange acting as a column; $M_{th} = M_u$.

Larger Portion of the Web in Tension (Q_1-Q_4-Q_5). -

(a) In the portion Q_1-Q_4, ($\sigma_{st} < \sigma_{yt}$), the panel is under high shear and relatively low moment. The panel behavior is similar to that of the portion Q_1-Q_2, described above.

(b) At point Q_4, the stress in the tension flange due to the ultimate web shear strength under combined loads is equal to the tension flange yield stress ($\sigma_{st} = \sigma_{yt}$) and the panel will fail simultaneously due to yielding of the tension flange and of the web plate.

(c) In the portion between Q_4 and Q_5, the panel is under shear and high moment. The tension flange starts yielding before the web

plate reaches its ultimate shear strength. Then, the yielding will penetrate into the web and finally cause the plastification of the cross section.

Based on the location of the neutral axis, the derivation of the ultimate strength equations can be separated into two cases.

Neutral Axis in the Web. - By assuming that the web under combined loads yields uniformly through the full depth, the average shear stress, as shown in Fig. 9 , is

$$\tau = \frac{V_{th}}{A_w} \tag{20a}$$

where V_{th} is the shear force under investigation. Substituting τ from Eq. 20a into the von Mises yield condition, the web stress due to bending is obtained.

$$\sigma = \sigma_{yw}\sqrt{1 - 3\left(\frac{V_{th}}{\sigma_{yw} A_w}\right)^2} \tag{20b}$$

By setting the sum of the normal forces, acting on the cross section shown in Fig. 9b, equal to zero, the location of the neutral axis of a fully yielded cross section is expressed in terms of nondimensional parameters η and ρ^*

$$\eta_g = 0.5 - \frac{0.5}{\rho_7}(\rho_1 \rho_4 - \rho_2 \rho_5) \tag{20c}$$

---

* ρ's and η's are defined in Appendix II (Notation).

The shear force and the moment which act at the center of the panel are then

$$V_{th} = \frac{\sqrt{3}\ V_p}{\mu} [\rho_1\ \rho_4\ (\eta_g + \eta_e) + \rho_7\ (\eta_g^2 - \eta_g + 0.5) \tag{20d}$$

$$+ \rho_2\ \rho_5\ (1 - \eta_g + \eta_f)]$$

and

$$M_{th} = \mu b\ V_{th} \tag{20e}$$

where the plastic shear force of the web, V_p, is

$$V_p = \tau_y\ A_w = \frac{1}{\sqrt{3}} \sigma_{yw}\ A_w \tag{20f}$$

Neutral Axis in the Compression Flange - The location of the neutral axis of a fully yielded cross section shown in Fig. 10 is

$$\eta_g = 0.5\ (\rho_1\ \rho_4 - \rho_7 - \rho_2\ \rho_5)\ \frac{1}{\rho_4\ \eta_h} \tag{21a}$$

The shear force V_{th} and the corresponding moment M_{th} acting at the center of the panel are

$$V_{th} = \frac{\sqrt{3}\ V_p}{\mu} [\rho_1\ \rho_4\ (\eta_e - \eta_g) + \rho_4\ \eta_h\ \eta_g^2$$

$$+ \rho_7\ (0.5 + \eta_g) + \rho_2\ \rho_5\ (1 + \eta_g + \eta_f)] \tag{21b}$$

and

$$M_{th} = \mu b \, V_{th} \tag{21c}$$

(d) At point Q_5, the panel is under pure bending. As shown in Ref. 8, the failure mechanism will be the plastification of the cross section,

$$M_{th} = M_p \tag{22}$$

where M_p is the plastic moment of the cross section.

Maximum Moment in Panel. - Since under combined loads the moment at one end of the panel is greater than the mid-panel moment for which the analysis is performed according to the above described procedure, it may happen that this maximum panel moment will control the panel strength. This is especially true for panels with large aspect ratios.

The shear producing the maximum panel moment may not exceed, depending on the case, one of the following values:

(a) Larger Portion of the Web in Compression (Q_1-Q_2-Q_3). -

$$V'_{th} \leq \frac{M_u}{\mu b + \frac{1}{2} a} \frac{\sigma_{yc}}{\sigma_{cf}} \tag{23a}$$

(b) Larger Portion of the Web in Tension (Q_1-Q_4-Q_5). -

$$V'_{th} \leq \frac{\sqrt{3}\, V_p}{\mu + \frac{1}{2}\alpha} [\rho_1 \rho_4 (\eta_g + \eta_e) + \rho_7 (\eta_g^2 - \eta_g + 0.5) + \rho_2 \rho_5 (1 - \eta_g + \eta_f)] \tag{23b}$$

or

$$V'_{th} \leq \frac{\sqrt{3}\ V_p}{\mu + \frac{1}{2}\alpha} [\rho_1\ \rho_4\ (\eta_e - \eta_g) + \rho_4\ \eta_h\ \eta_g^2$$

$$+ \rho_7\ (0.5 + \eta_g) + \rho_2\ \rho_5\ (1 + \eta_g + \eta_f)] \qquad (23c)$$

for the neutral axis in the web or in the compression flange, respectively. These two equations (Eqs. 23b and 23c) are simply Eqs. 20d and 21b modified for an increased shear span (from μb to $\mu b + \frac{1}{2} a$).

It seems reasonable and sufficiently accurate, mostly on the safe side, to simplify the maximum panel moment limitation to keeping it below the moment which would produce yielding according to the ordinary beam theory.

$$V'_{th} \leq \frac{I\ \sigma_{yf}}{y\ b\ (\mu + \frac{1}{2}\alpha)} \qquad (24)$$

where σ_{yf} is the yield stress and y is the distance from the centroid to the flange for either the compression or tension flange, whichever gives the smaller V'_{th} and thus controls.

4. COMPARISON WITH TEST RESULTS

The ultimate strength theory was checked against the available fifty - three tests on symmetrical plate girders,[1,5,9,10,17,18,21] hybrid girders,[13,16] and unsymmetrical plate girders.[12,23] Tables 1 to 3 summarize the dimensions of the test panels, material properties, the experimental ultimate loads, the ultimate loads from the theoretical analysis, as well as a comparison between the experimental and predicted ultimate loads. The test load is shown on the theoretical interaction curves for each individual panel in Figs. 11 to 24.

Symmetrical girders with homogeneous material properties are given in Table 1 and the interaction curves for each panel are shown in Figs. 11 to 16. The mode of failure of all these panels except for one is classified as the web failure (shear failure). The average deviation of the available thirty-one test loads is 4% with the maximum deviation of 12% (G4 in Reference 18).

The comparison of the theory with tests on unsymmetrical plate girders is made in Table 2 and Figs. 17 to 20. The tests on panels with the smaller flange and, thus, the larger portion of the web, in compression and failing in the web are shown in Table 2(a). The interaction diagrams are in Figs. 17 and 18 (UG2.2 and UG4.1). The theory gives an over-estimate of 1%.

Table 2(b) gives the girder panels with the smaller flange in compression and subjected to high shear and high moment. The panel strength for these cases was limited by the failure of the compression flange.

The interaction curves for these tests are shown in Figs. 17, 18 and 19 where the reduction of the panel bending carrying capacity due to the effect of shear, is illustrated. An average of 6% underestimate is obtained for the four tests with the extreme deviation of 10% underestimate.

The girder panels with the smaller flange in tension and subjected primarily to shear are given in Table 2(c). The interaction curves are in Figs. 18 and 19. The mode of failure is classified as the web failure. An average deviation of 5% is obtained for the available three tests with the maximum deviation of 12%.

A comparison of the test results for symmetrical hybrid girders with the predictions of the proposed approach is shown in Table 3. The interaction curves for the individual tested panels are given in Figs. 21 to 24. An average deviation from the available thirteen tests is 7% with the maximum deviation of 15%.

A comparison for girder panels with the same geometrical and material properties, but subjected respectively to pure shear, a combination of shear and moment, and pure moment is shown in Fig. 20. A good agreement between the test results and the computed values is observed.

The overall average deviation of the available fifty - three test results (Tables 1 to 3) is 5% with the extreme deviation of 15%

A comparison of some test results for unsymmetrical plate girders with the proposed approach and with the approaches currently

available (1970) is shown in Fig. 25. As in all previous plots, the ordinate gives the shear force divided by the pure ultimate shear V_u obtained by the proposed approach and the abscissa gives the moment divided by the pure ultimate moment M_u. The test results for three unsymmetrical panels, identical in all respects except for the type of loading, are shown by the heavy dots. The interaction diagram according to the proposed approach is represented by curve (1). The methods of References 2 and 4 were adjusted following the reasoning of Reference 24 to make them applicable to unsymmetrical girders and the corresponding interaction diagrams are given by curves (2) and (3). The vertical line (4) represents a cut-off on the moment capacity given by curve (3) and thus limits safe designs to the region indicated by cross hatching. The interaction diagram of Reference 24, curve (5), is the most conservative of those shown. The method of Reference 1 is not included because it is not applicable to unsymmetrical sections and cannot be readily modified as was done here for the methods of References 2 and 4. It is seen in the figure that the proposed approach gives the most consistent correlation with the test results.

Comparisons of interaction diagrams for panels of other dimensions were also made and they consistently showed a greater accuracy of the proposed method than of others.

5. CONCLUSIONS

The conclusions drawn as a result of this investigation are the following:

1. The ultimate strength of an unsymmetrical plate girder panel depends on the direction of the moment which acts on the panel, that is, whether the larger portion of the web is in tension or in compression. The panel capacity is greater when the larger portion of the web is in tension.

2. The ultimate strength of a plate girder panel under combined loads may be of two types: the shear capacity is reduced by bending when the panel is subjected primarily to shear, and the bending capacity is reduced by shear when the panel is subjected primarily to bending.

3. The proposed approach gives a reliable means of determining the ultimate strength of homogeneous or hybrid girders with symmetrical or unsymmetrical cross section. It is, however, too complicated for manual computations and a computer must be employed. In the fufute, the numerical output from the computer program should be used to evolve simple formulas suitable for practical design.

6. ACKNOWLEDGEMENTS

This report was prepared as part of a research project on unsymmetrical plate girders conducted in the Department of Civil Engineering, Fritz Engineering Laboratory, Lehigh University, Bethlehem, Pennsylvania. Dr. David A. VanHorn is Chairman of the Department and Dr. Lynn S. Beedle is Director of the Laboratory.

The authors express their gratitude to the American Iron and Steel Institute, the Pennsylvania Department of Transportation, the Federal Highway Administration of the U. S. Department of Transportation, and the Welding Research Council for supporting this project. They also gratefully acknowledge the technical guidance provided by the Welded Plate Girder Subcommittee of the Welding Research Council under the consecutive chairmanship of Mr. M. Deuterman, E. G. Paulet, and G. F. Fox and by the Task Group on Unsymmetrical Plate Girders under the chairmanship of Mr. C. A. Zwissler and, lately, Mr. L. H. Daniels.

The detailed review of the report made by Messrs. H.G. Juhl and J. Nishanian, respectively, of the Pennsylvania Department of Transportation and the Federal Highway Administration is sincerely appreciated.

Appreciation is due to Mrs. A. Brumbelow for typing and to Mr. J. M. Gera for drafting.

7. APPENDIX I - REFERENCES

1. Akita, Y., and Fujii, T.
ON ULTIMATE STRENGTH OF PLATE GIRDERS, Japan Shipbuilding and Marine Engineering, May, 1968.

2. American Institute of Steel Construction
SPECIFICATION FOR THE DESIGN, FABRICATION AND ERECTION OF STRUCTURAL STEEL FOR BUILDINGS, AISC, New York, 1969.

3. Basler, K.
STRENGTH OF PLATE GIRDERS, Ph.D. Dissertation, Lehigh University, 1959, available from University Microfilms, Ann Arbor, Michigan.

4. Basler, K.
STRENGTH OF PLATE GIRDERS IN COMBINED BENDING AND SHEAR, Proceedings ASCE, Vol. 87, ST7, Part 1, October, 1961.

5. Basler, K., Yen, B. T., Mueller, J. A., and Thurlimann, B.
WEB BUCKLING TESTS ON WELDED PLATE GIRDERS, Welding Research Council, Bulletin No. 64, Sept., 1960.

6. Bergfelt, A., and Hovik, J.
THIN-WALLED DEEP PLATE GIRDERS UNDER STATIC LOADS, Final Report of the 8th Congress of the International Association for Bridge and Structural Engineering, held in New York, Sept., 1968, ETH, Zurich.

7. Chern, C., and Ostapenko, A.
ULTIMATE STRENGTH OF PLATE GIRDERS UNDER SHEAR, Fritz Engineering Laboratory Report No. 328.7, Lehigh University, Sept. 1969.

8. Chern, C., and Ostapenko, A.
BENDING STRENGTH OF UNSYMMETRICAL PLATE GIRDERS, Fritz Engineering Laboratory Report No. 328.8, Lehigh University, Sept., 1970.

9. Cooper, P. B.
BENDING AND SHEAR STRENGTH OF LONGITUDINALLY STIFFENED PLATE GIRDERS, Ph.D. Dissertation, Lehigh University, 1965, available from University Microfilms, Ann Arbor, Michigan.

10. Cooper, P. B., Lew, H. S., and Yen, B. T.
WELDED CONSTRUCTIONAL ALLOY STEEL PLATE GIRDERS, Proceedings, ASCE, V90, ST11, Part I, Feb., 1964.

11. Cooper, P. B.
PLATE GIRDERS, Chapter 8 in STRUCTURAL STEEL DESIGN, by L. Tall, et al., Ronald Press, New York, 1964.

12. Dimitri, J. R. and Ostapenko, A.
PILOT TESTS ON THE ULTIMATE STATIC STRENGTH OF UNSYMMETRICAL PLATE GIRDERS, Fritz Engineering Laboratory Report No. 328.5, Lehigh University, June, 1968.

13. Fielding, D. J., and Toprac, A. A.
FATIGUE TESTS OF HYBRID PLATE GIRDERS UNDER COMBINED BENDING AND SHEAR, Research Report No. 96-2, Center for Highway Research, The University of Texas, Austin, Texas, July 1967.

14. Fujii, T.
ON AN IMPROVED THEORY FOR DR. BASLER'S THEORY, Final Report of the 8th Congress of the International Association for Bridge and Structural Engineering, held in New York, Sept., 1968, ETH, Zurich.

15. Kollbrunner, C. F. and Meister, M.
AUSBEULEN, Springer-Verlag, Berlin, 1958.

16. Lew, H. S. and Toprac, A. A.
THE STATIC STRENGTH OF HYBRID PLATE GIRDERS, Report No. S.F.R.L. RPT. P550-11, Structural Fatigue Research Laboratory, Department of Civil Engineering, The University of Texas, Austin, Jan., 1968.

17. Lyse, I. and Godfrey, H. J.
INVESTIGATION OF WEB BUCKLING IN STEEL BEAMS, Trans. ASCE, Vol. 100, 1935.

18. Nishino, F. and Okumura, T.
EXPERIMENTAL INVESTIGATION OF STRENGTH OF PLATE GIRDERS IN SHEAR, Final Report of the 8th Congress of the International Association for Bridge and Structural Engineering, held in New York, Sept., 1968, ETH, Zurich.

20. Owen, D. R. J., Rockey, K. C., and Skaloud, M.
BEHAVIOR OF LONGITUDINALLY REINFORCED PLATE GIRDERS, Final Report of the 8th Congress of the International Association for Bridge and Structural Engineering, held in New York, Sept., 1968, ETH, Zurich.

21. Patterson, P. J., and Yen, B. T.
PROOF-TESTS OF TWO PLATE GIRDERS FOR DESIGN RECOMMENDATIONS, Fritz Engineering Laboraotry Report No. 327.7, Lehigh University, June, 1969.

22. Rockey, K. C., and Skaloud, M.
INFLUENCE OF FLANGE STIFFNESS UPON THE LOAD CAPACITY OF WEBS IN SHEAR, Final Report of the 8th Congress of the International Association for Bridge and Structural Engineering, held in New York, Sept., 1968, ETH, Zurich.

23. Schueller, W., and Ostapenko, A.
MAIN TESTS ON THE ULTIMATE STATIC STRENGTH OF UNSYMMETRICAL PLATE GIRDERS, Fritz Engineering Laboratory Report No. 328.6, Lehigh University, Aug., 1968.

24. Vincent, G. S.
TENTATIVE CRITERIA FOR LOAD FACTOR DESIGN OF STEEL HIGHWAY BRIDGES, American Iron and Steel Institute, Bulletin No. 15, March 1969.

8. APPENDIX II. - NOTATION

1. Lower Case Letters

a	Panel width, that is, distance between transverse stiffeners.
b	Panel depth, that is, distance between flanges.
c_c	Half width of the compression flange.
c_t	Half width of the tension flange.
d_c	Thickness of the compression flange.
$\bar{d}_c$	Distance from the compression flange-web junction to the centroid of the compression flange.
d_f	Thickness of the tension flange.
$\bar{d}_t$	Distance from the tension flange-web junction to the centroid of the tension flange.
k_b	Plate buckling coefficient under pure bending.
k_v	Plate buckling coefficient under pure shear.
m_{cl}, m_{cr}, m_{tl}, m_{tr}	Plastic moments developed in the compression and tension flanges at the left and right sides of the panel due to the frame action under combined loads.
t	Web thickness
$x = \frac{M_{max}}{V}$	Shear span, that is, the location of the far end of the panel relative to the point of zero moment.
y_c	Distance from the neutral axis to the extreme compression fiber of the web before buckling.
y_o	Distance from the neutral axis to the compression flange-web junction for a fully yielded cross section.
y_s	Distance from the neutral axis to the extreme tensile fiber

2. Upper Case

A	Area of the plate girder cross section.
A_{fc}	Area of the compression flange.
A_{ft}	Area of the tension flange.
A_w	Area of the web.
C	The ratio of the maximum tensile stress (or minimum compressive stress) to the maximum compressive stress of the web plate (for a positive moment, C is the ratio of the bottom fiber stress to the top fiber stress). Note that C is negative when the bottom fiber is in tension.
E	Modulus of elasticity,
H	Horizontal component of the tension field force; H', for incomplete tension field.
I	Moment of inertia of the cross section about the horizontal centroidal axis,
M	Moment.
M_{max}	Maximum moment in panel.
M_p	Plastic moment,
M_{th}	Moment acting on the panel under V_{th}.
M_u	Ultimate moment controlled by the capacity of the compression flange, pure bending.
R	Parameter used in Eq.7.
S	Average stress in the tension portion of the web at buckling.
V	Shear.

V_p Plastic shear of the web.

V_{th} Ultimate shear strength of the panel under combined loads.

V_τ Beam action shear; with subscript "τc", under combined loads.

V_f Frame action shear; with subscript "fc", under combined loads.

V_σ Tension field action shear; with subscript "σc", under combined loads.

V'_σ Incomplete tension field shear under combined loads.

3. Greek Letters

$\alpha = a/b$ Aspect ratio, that is, panel length to depth ratio.

$\beta = b/t$ Web slenderness ratio, that is, web depth to thickness ratio.

δ Parameter defined for Eq.7.

ε Strain; with subscript "y", yield strain.

ζ Coefficient of effective web depth.

$\eta_e, \eta_f, ..$ Non-dimensional parameters: $\eta_e = \bar{d}_c/b$, $\eta_f = \bar{d}_t/b$, $\eta_g = y_o/b$, $\eta_h = \frac{2c_c}{t}$

$\mu = \frac{M}{bV}$ Shear span ratio.

ν Poisson's ratio.

ρ Coefficient of equivalent tension field stress in the elastic triangular portion.

$\rho_1, \rho_2, ..$ Non-dimensional parameters: $\rho_1 = A_{fc}/A_w$, $\rho_2 = A_{ft}/A_w$, $\rho_4 = \sigma_{yc}/\sigma_{yw}$, $\rho_5 = \sigma_{yt}/\sigma_{yw}$, $\rho_7 = \sigma/\sigma_{yw}$

σ_{1c}, σ_{2c}, σ_{3c}, σ_{sc}	Reference stresses in the compression flange.
σ_{1t}, σ_{2t}, σ_{3t}, σ_{st}	Reference stresses in the tension flange.
σ_{bc}	Bending buckling stress under combined loads.
σ_{cf}	Critical stress of the compression flange column.
σ_{cp}	Plate buckling stress under pure bending.
σ_t	Tension field stress in the fully yielded zone; with subscript "c", under combined loads.
σ_{yc}	Yield stress of the compression flange.
σ_{yt}	Yield stress of the tension flange.
σ_{yw}	Yield stress of the web.
τ_c	Shear buckling stress under combined loads.
τ_{cr}	Theoretical shear buckling stress under pure shear.
ϕ	Inclination of the tension field; with subscript "c", under combined loads;with subscript "o", the optimum inclination of the tension field.
Ω	Ratio of the horizontal component to the vertical component of the tension field force.

In general, subscript "ex" (experimental) refers to ultimate loads, moments, and shears observed in tests.

9. TABLES AND FIGURES

Table 1. Comparison with Tests on Symmetrical Plate Girders

Source	Test No.	α	β	Web		Compression Flange		Tension Flange		$\mu = \frac{M_{ex}}{V_{ex} b}$	V_{ex}	V_{th}	$\frac{V_{ex}}{V_{th}}$
				b x t	σ_{yw}	$2c_c \times d_c$	σ_{yc}	$2c_t \times d_t$	σ_{yt}				
(1)	(2)	(3)	(4)	(5)	(6)	(7)	(8)	(9)	(10)	(11)	(12)	(13)	(14)
				in. x in.	Ksi	in. x in.	Ksi	in. x in.	Ksi		Kips	Kips	
Ref. 5	G8-T1	3.0	254	50.0 x .197	38.2	12.0 x .752	41.3	12.0 x .747	41.3	1.5	85	87.2	.98
	G8-T3	1.5	"	"	"	"	"	"	"	2.25	116.5	117.2	.99
	G9-T3	"	382	50.0 x .131	44.5	12.0 x .755	41.8	12.0 x .745	41.8	2.25	79	83.5	.95
Ref.10	H1-T1	3.0	127	50.0 x .393	108.1	*17.03 x .982 18.06 x .977	102.0	*17.03 x .982 18.06 x .983	102.0	1.25	630	610	1.03
	H1-T2	1.5	"	"	"	18.06 x .977	"	18.06 x .983	"	0.75	769	770	1.00
	H2-T1	1.0	128	50.0 x .390	110.2	*17.06 x 1.008 18.06 x 1.008	108.8	*17.06 x 1.008 18.06 x 1.008	108.8	2.5	917	971	.95
	H2-T2	0.5	"	"	"	"	"	"	"	2.75	1125	1235	.91
Ref. 9	LS1-T1	1.0	256	50.0 x .195	46.8	14.12 x 1.498	30.5	14.12 x 1.498	30.5	2.5	182	181	1.00
Ref.21	F10-T1	1.5	197	50.0 x .254	38.7	16.0 x 1.018	30.2	16.0 x 1.018	30.2	2.43	170	174.6	.97
	F10-T2	"	"	"	"	"	"	"	"	1.23	184	184.0	1.00
	F10-T3	1.2	"	"	"	"	"	"	"	1.08	190	202	.94
Ref.17	WB-1	2.64	56	14.0 x .248	43.3	10.0 x 1.55	33.0	10.0 x 1.55	33.0	1.32	109	109	1.00
	WB-2	"	55	14.0 x .255	47.8	10.0 x 1.56	"	10.0 x 1.56	"	1.32	128	119.5	1.07
	WB-3	2.56	59	16.03 x .273	49.6	10.06 x 1.50	"	10.06 x 1.50	"	1.28	139	140.5	.99
	WB-6	2.45	70	17.56 x .251	33.1	10.02 x 1.51	"	10.02 x 1.51	"	1.23	96	100	.96
	WB-7	2.51	61	15.34 x .253	33.7	10.07 x 1.50	"	10.07 x 1.50	"	1.26	95	98	.97
	WB-8	2.46	60	15.65 x .262	29.7	10.07 x 1.51	"	10.07 x 1.51	"	1.23	100	97.5	1.03
	WB-9	2.68	50	12.50 x .250	30.3	10.04 x 1.50	"	10.04 x 1.50	"	1.34	92	92	1.00
	WB-10	"	"	12.50 x .252	"	10.01 x 1.51	"	10.01 x 1.51	"	1.34	94	92.5	1.01

* Cover plate welded to the flange.

Continued

Table 1. Comparison with Tests on Symmetrical Plate Girders (Continuation)

Source	Test No.	α	β	Web		Compression Flange		Tension Flange		$\mu = \frac{M_{ex}}{V_{ex}b}$	V_{ex}	V_{th}	$\frac{V_{ex}}{V_{th}}$
				b x t	σ_{yw}	$2c_c \times d_c$	σ_{yc}	$2c_t \times d_t$	σ_{yt}				
(1)	(2)	(3)	(4)	(5)	(6)	(7)	(8)	(9)	(10)	(11)	(12)	(13)	(14)
				mm x mm	kg/mm^2	mm x mm	kg/mm^2	mm x mm	kg/mm^2		Tons	Tons	
Ref.1	G1	2.61	55	440 x 8.0	44.0	160 x 30	42.0	160 x 30	42.0	1.31	82	91	.90
	G2	"	"	"	"	200 x 30	"	200 x 30	"	1.31	84	93.5	.92
	G3	2.63	70	560 x 8.0	"	160 x 30	"	160 x 30	"	1.31	99	107.6	.92
	G4	3.68	"	"	"	250 x 30	"	250 x 30	"	1.84	97	101.2	.95
	G5	2.68	"	"	"	"	"	"	"	1.34	107	111	.97
	G6	1.25	"	"	"	"	"	"	"	1.88	120	123.5	.97
	G7	2.68	"	"	"	"	"	"	"	1.34	107	111	.97
	G9	2.78	90	720 x 8.0	"	"	"	"	"	1.39	118	125	.95
Ref.18	G1	2.67	59.7	543 x 9.1	38.0	301 x 22.4	44.0	301 x 22.4	44.0	1.34	110.5	110	1.00
	G2	"	"	"	"	220 x 22.4	"	220 x 22.4	"	1.34	104	108	.96
	G3	2.63	76.8	722 x 9.4	"	302 x 22.2	"	302 x 22.2	"	1.31	124.5	137	.91
	G4	"	"	"	"	243 x 22.2	"	243 x 22.2	"	1.31	114.5**	131	.88

* Cover plate welded to the flange.

** Failure of the flange.

Table 2. Comparison with Tests on Unsymmetrical Plate Girders.

Source	Test No.	α	β	Web		Compression Flange		Tension Flange		$\mu = \frac{M_{ex}}{V_{ex} b}$	V_{ex}	V_{th}	$\frac{V_{ex}}{V_{th}}$
				b x t	σ_{yw}	$2c_c \times d_c$	σ_{yc}	$2c_t \times d_t$	σ_{yt}				
(1)	(2)	(3)	(4)	(5)	(6)	(7)	(8)	(9)	(10)	(11)	(12)	(13)	(14)
				in. x in.	Ksi	in. x in.	Ksi	in. x in.	Ksi		Kips	Kips	
(a) Smaller Flange in Compression -- Failure of the Web													
Ref.12	UG2.2	1.2	295	36.0 x .122	43.2	8.0 x .625	36.7	8.0 x .625 *10.5 x .750	36.7	1.39	70	70.5	0.99
Ref.23	UG4.1	1.77	414	48.07 x .116	56.1	10.0 x .750	34.1	13.0 x 1.384	34.1	0.88	81.6	82.5	0.99
(b) Smaller Flange in Compression -- Failure of the Compression Flange													
Ref.12	UG3.2	1.6	295	36.0 x .122	43.5	8.0 x .625	33.3	8.0 x .625 *10.5 x .750	33.3	3.86	43.8	39.4	1.10
	UG3.3	"	"	"	"	"	"	"	"	3.86	42.5	"	1.07
Ref.23	UG4.3	1.46	414	48.07 x .116	56.1	10.0 x .750	34.1	13.0 x 1.384	34.1	3.77	63.2	60.0	1.05
	UG4.4	1.77	263	48.07 x .183	35.5	"	"	"	"	3.62	70	68.0	1.03
(c) Smaller Flange in Tension -- Failure of the Web													
Ref.23	UG4.2	1.14	414	48.07 x .116	56.1	13.0 x 1.384	34.1	10.0 x .750	34.1	1.93	119.2	106.0	1.12
	UG4.5	.83	263	48.07 x .183	35.5	"	"	"	"	2.19	136	133.5	1.02
	UG4.6	1.77	"	"	"	"	"	"	"	0.88	98.8	100.0	0.99

* Cover plate welded to the flange.

Table 3. Comparison with Tests on Symmetrical Hybrid Plate Girders.

Source	Test No.	α	β	Web		Compr. Flange		Tension Flange		$\mu = \frac{M_{ex}}{V_{ex} b}$	V_{ex}	V_{th}	$\frac{V_{ex}}{V_{th}}$
				b x t	σ_{yw}	$2c_c \times d_c$	σ_{yc}	$2c_t \times d_t$	σ_{yt}				
(1)	(2)	(3)	(4)	(5)	(6)	(7)	(8)	(9)	(10)	(11)	(12)	(13)	(14)
				in. x in.	Ksi	in. x in.	Ksi	in. x in.	Ksi		Kips	Kips	
Ref.16	HS1-T1	2.0	185.6	36.0 x .194	65.6	8.0 x .517	107.6	8.0 x .517	107.6	1.0	140	135	1.04
	HS1-T2	1.0	"	"	"	"	"	"	"	1.5	190	173.5	1.09
	HS1-T3	.5	"	"	"	"	"	"	"	1.75	226	214	1.05
	HS1A-T1	2.0	192	35.87 x .187	49.0	7.99 x .533	104.2	7.99 x .533	104.2	1.0	98	104	.94
	HS1A-T2	1.0	"	"	"	"	"	"	"	1.5	125	137	.96
	HS1A-T3	.5	"	"	"	"	"	"	"	1.75	167	158.5	1.05
	HS2-T1	2.0	182	36.0 x .198	54.6	8.0 x .517	107.6	8.0 x .517	107.6	1.0	131	122	1.07
	HS2-T2	1.0	"	"	"	"	"	"	"	1.5	177	153.5	1.15
	HS2-T3	.5	"	"	"	"	"	"	"	1.75	205	186.5	1.10
	31020	.83	190	36.0 x .189	40.8	8.02 x .522	105.0	8.02 x .522	105.0	2.08	115.8	115.8	1.00
	31530	"	"	"	"	7.99 x .528	"	7.99 x .528	"	2.08	108.1	115.5	.94
Ref.13	32550-C2	1.0	176.5	36.0 x .204	51.2	7.98 x .532	106.2	7.98 x .532	106.2	2.5	153	139.5	1.09
	32550-C2R	"	"	"	"	"	"	"	"	2.5	148	139.5	1.06

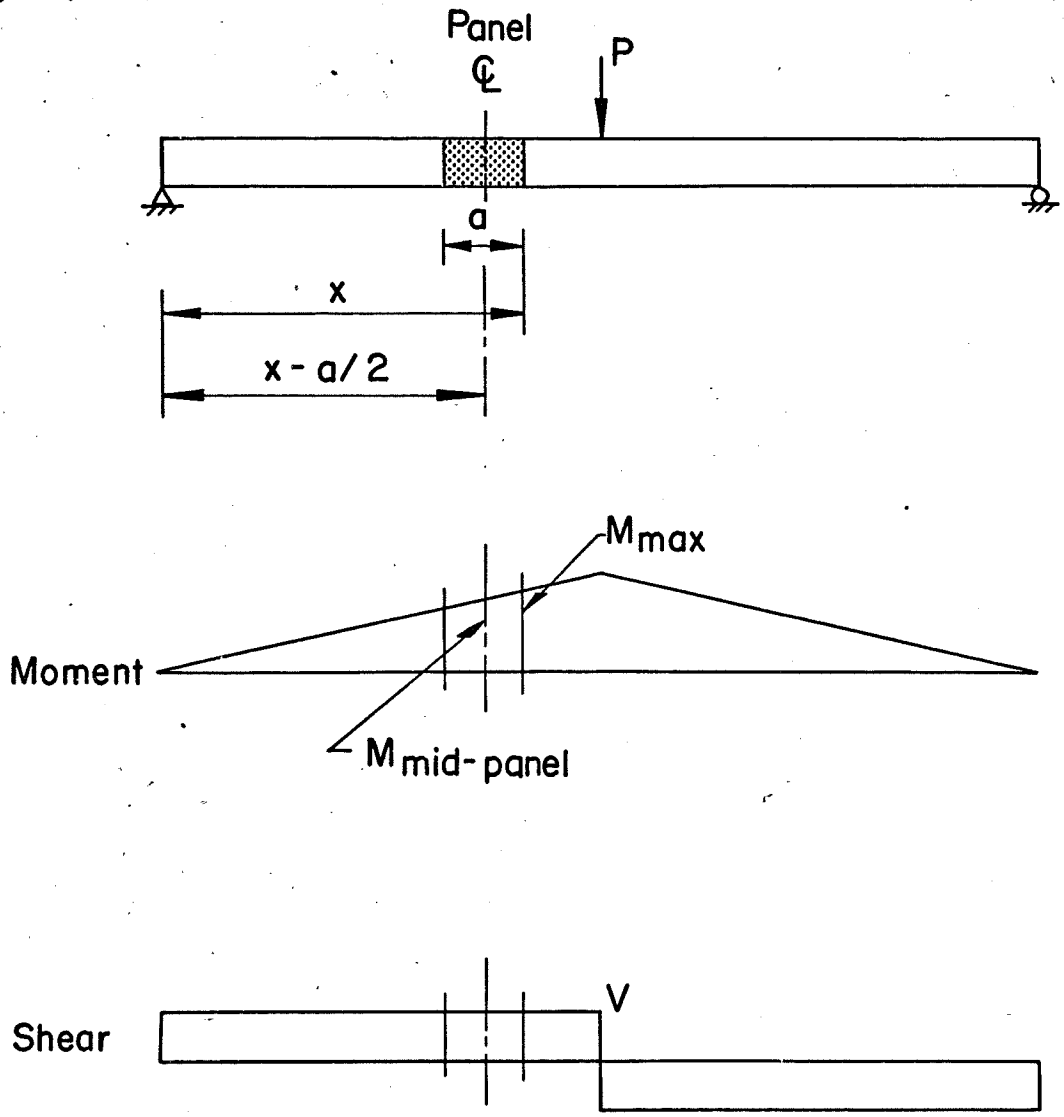

Fig. 1 Loading Diagram of the Panel Under Investigation

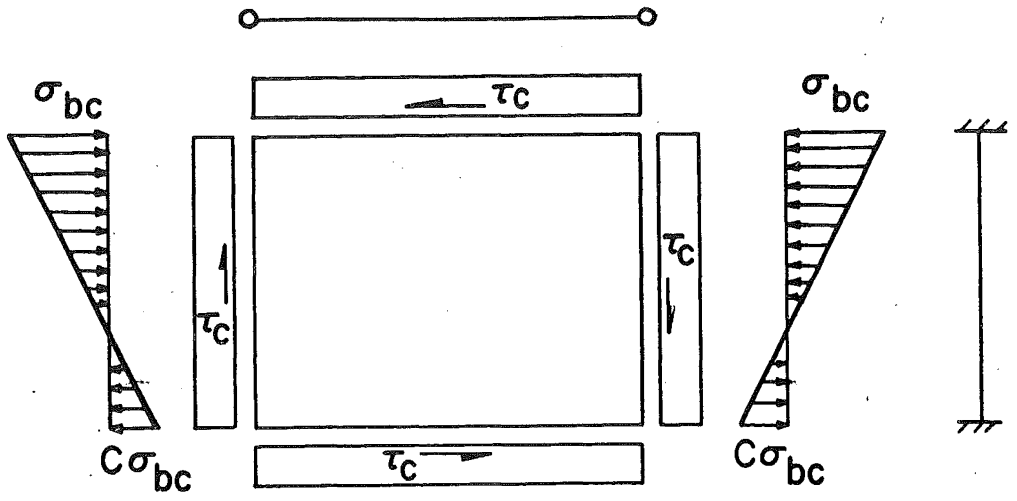

Fig. 2 Beam Action Model Under Combined Loads

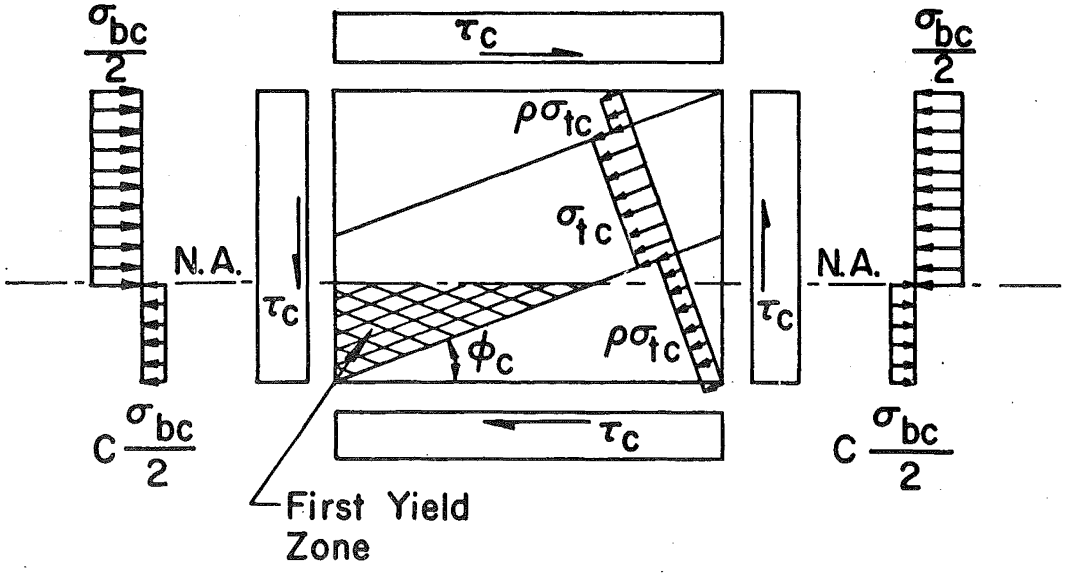

Fig. 3 Idealized Tension Field Model Under Combined Loads

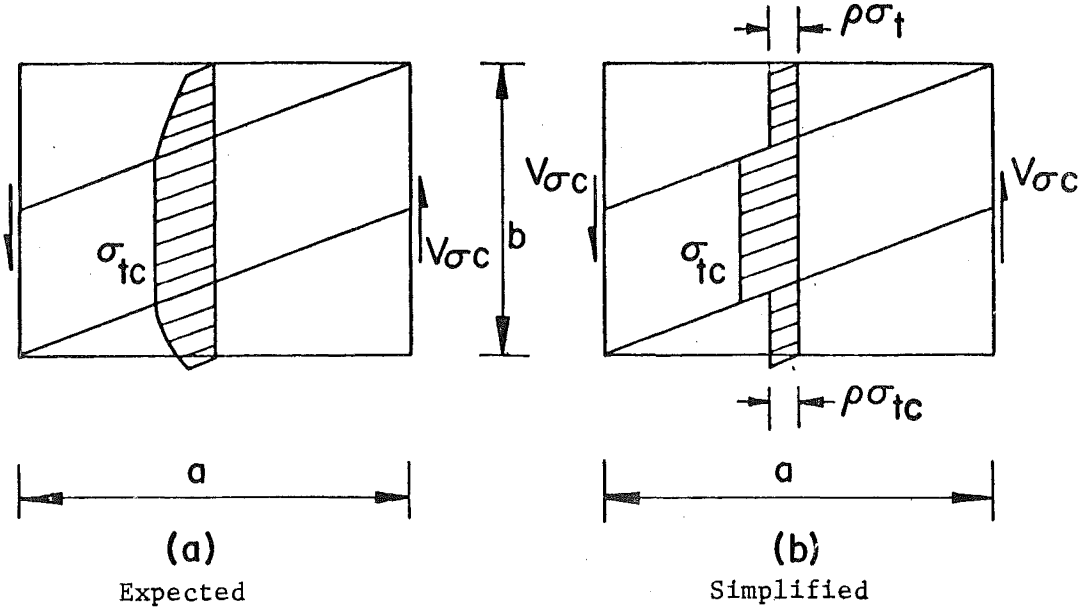

Fig. 4 Tension Field Stress Distribution Under Combined Loads

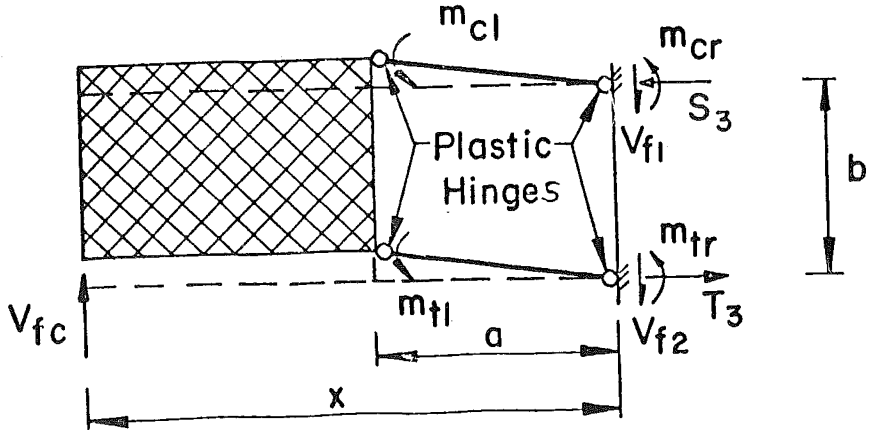

Fig. 5 Frame Action Model Under Combined Loads

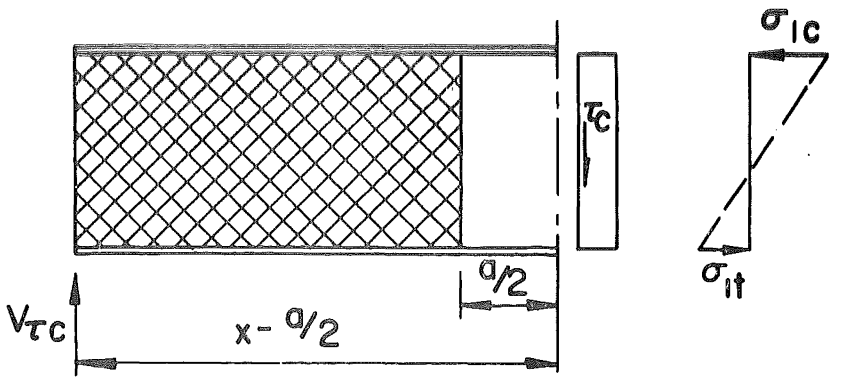

(a) Beam Action

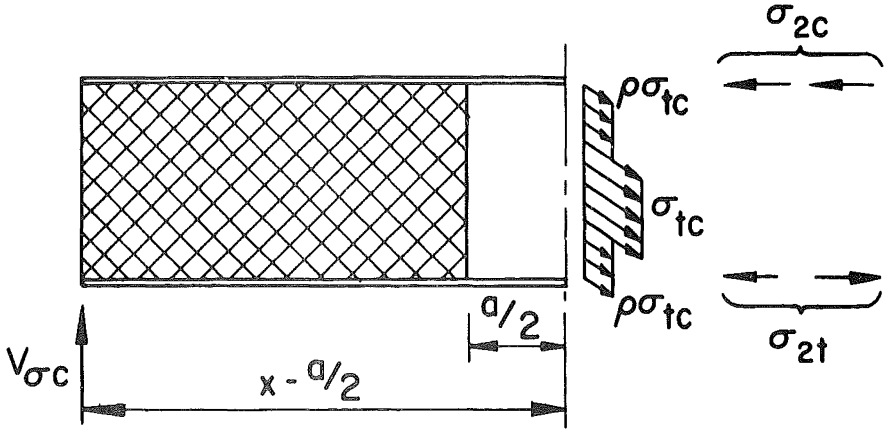

(b) Tension Field Action

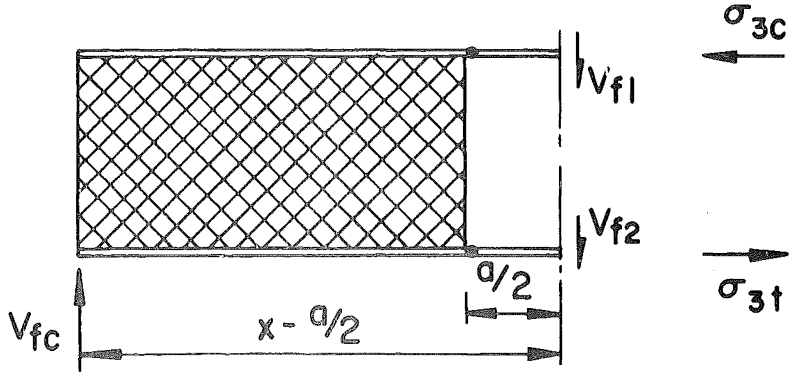

(c) Frame Action

Fig. 6 Reference Stresses in the Flanges

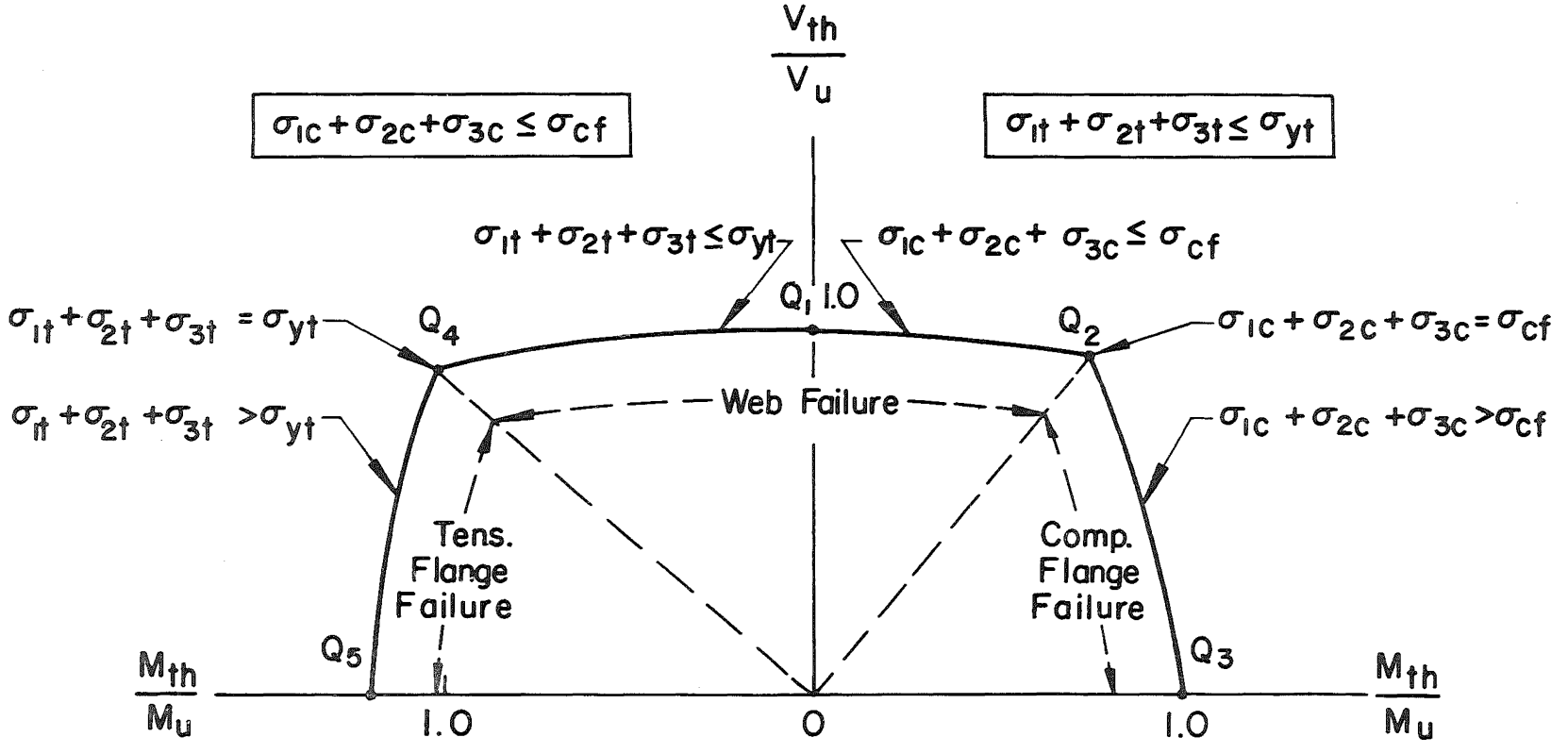

Fig. 7 Schematic Interaction Curve - Stress Inequality Relationships

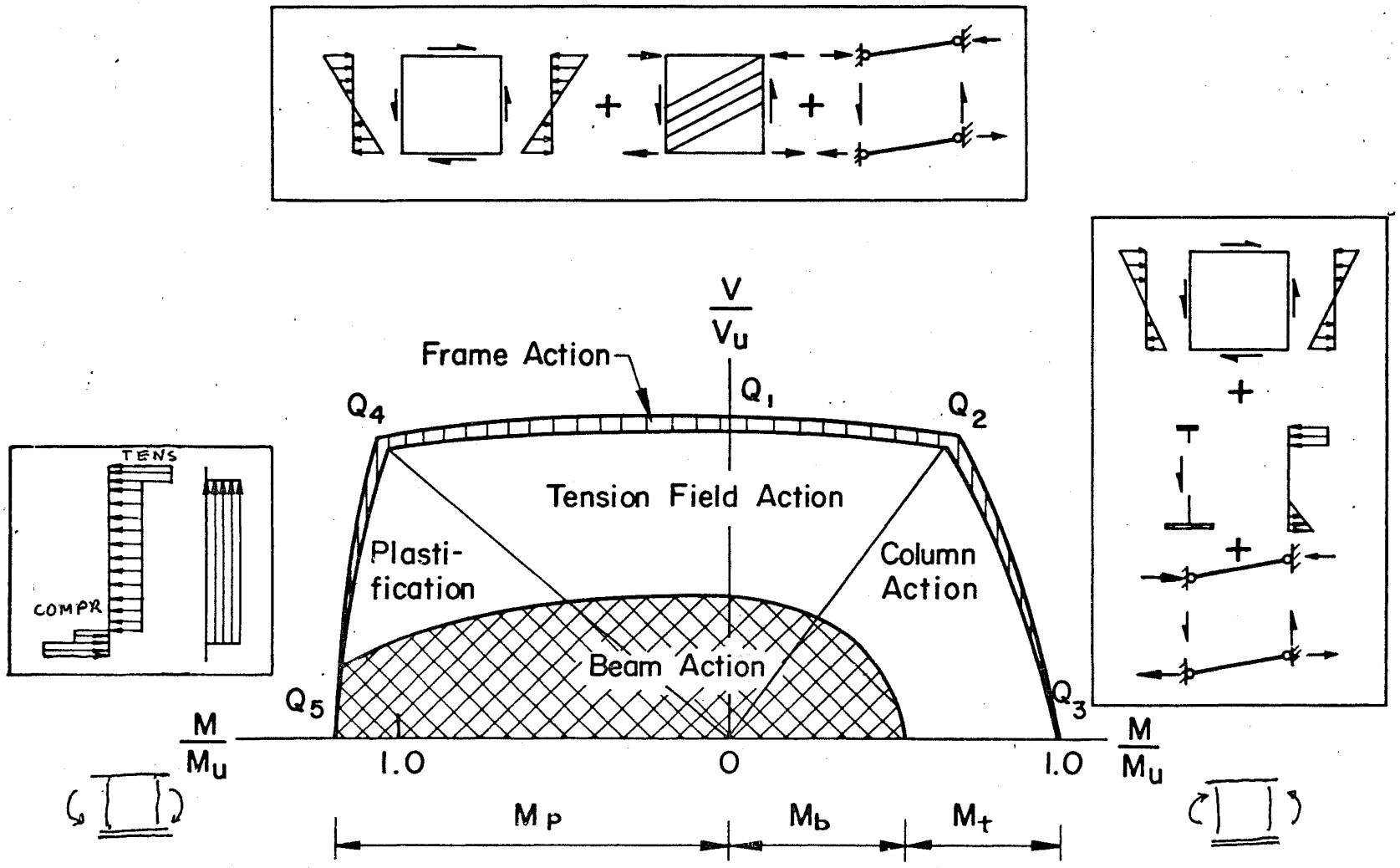

Fig. 8 Schematic Interaction Curve - Failure Mechanisms

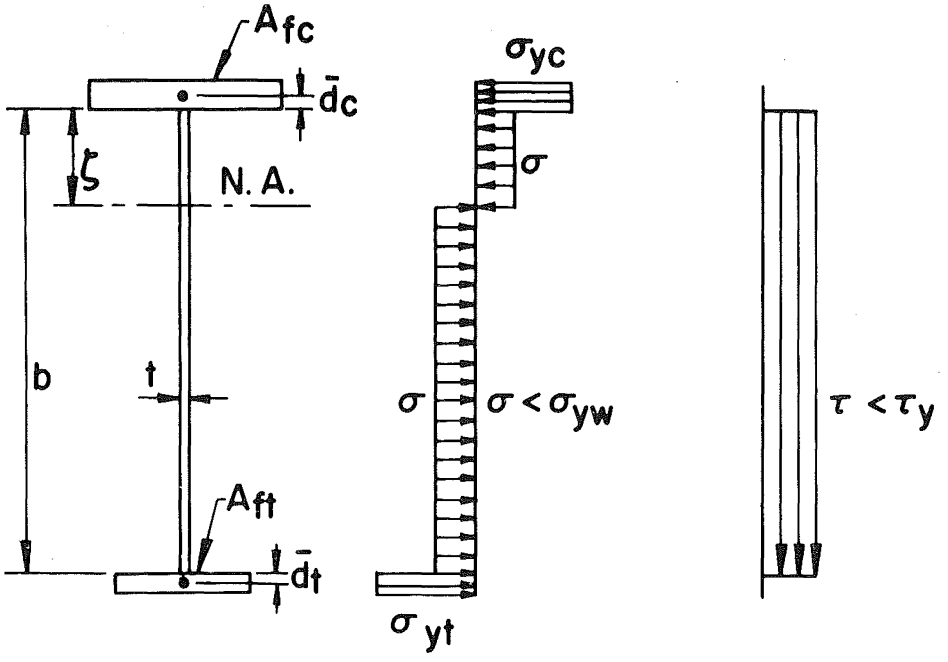

Fig. 9 Stress Distribution of Plastified Cross Section - Neutral Axis in the Web

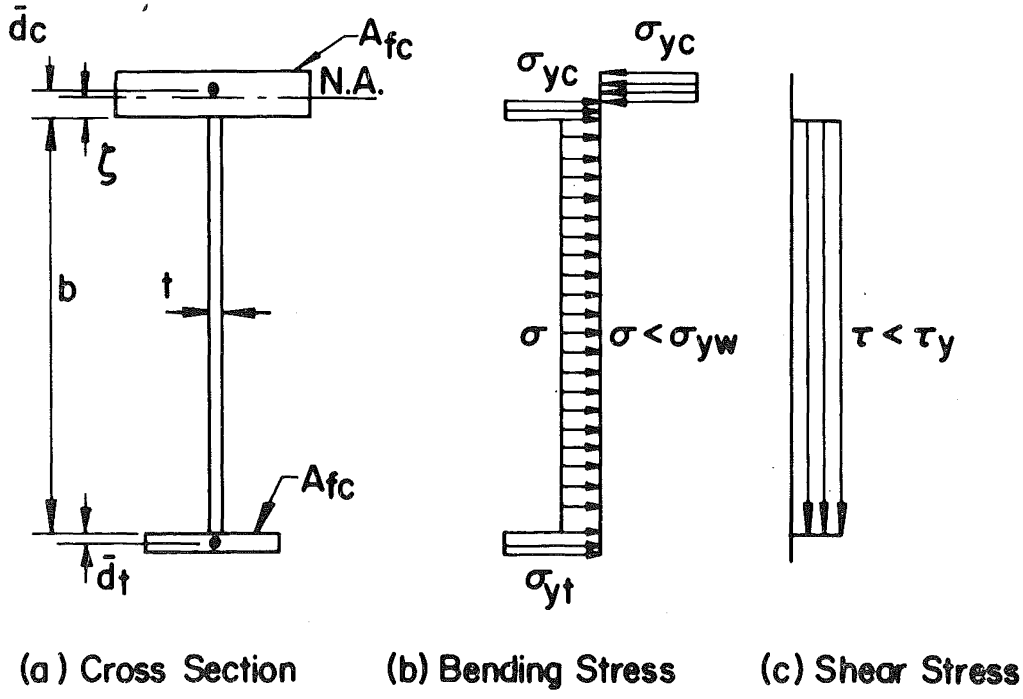

Fig. 10 Stress Distribution of Plastified Cross Section - Neutral Axis in the Flange

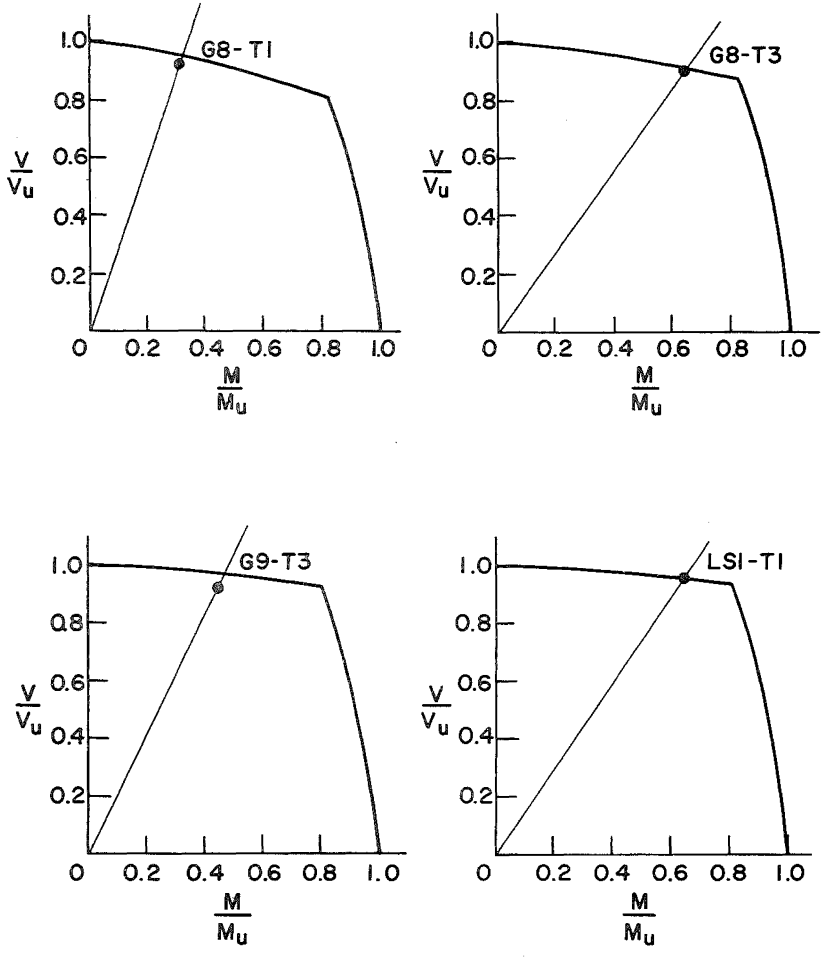

Fig. 11 Interaction Curves and Test Results - G8,G9 and LS1-T1 (Ref. 5 & 9)

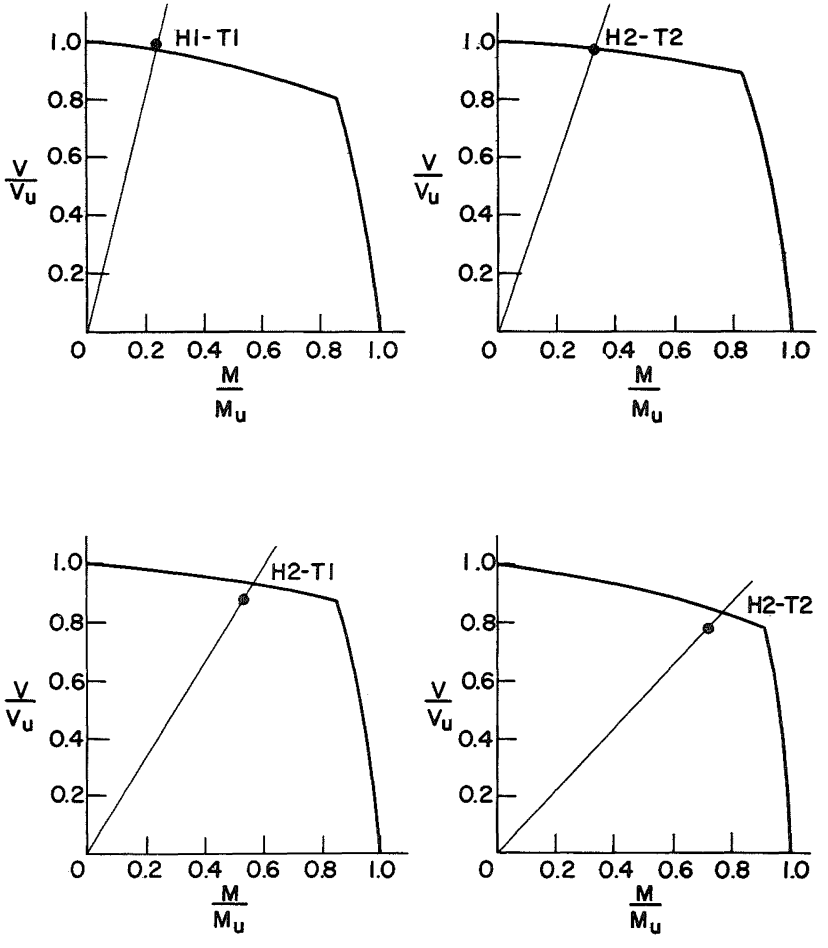

Fig. 12 Interaction Curves and Test Results - H1 and H2 Series (Ref. 10)

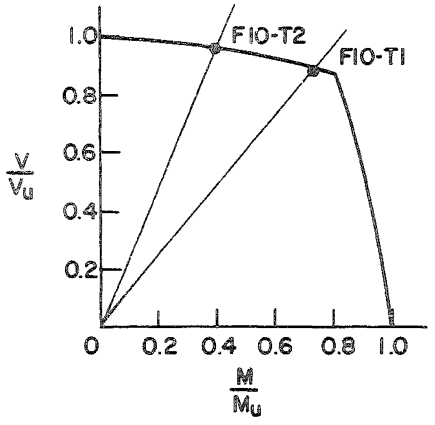

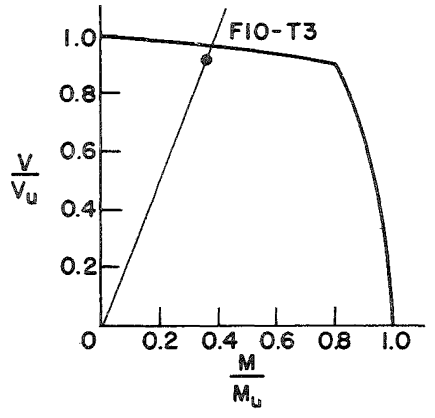

Fig. 13 Interaction Curves and Test Results - F10 Series (Ref 21)

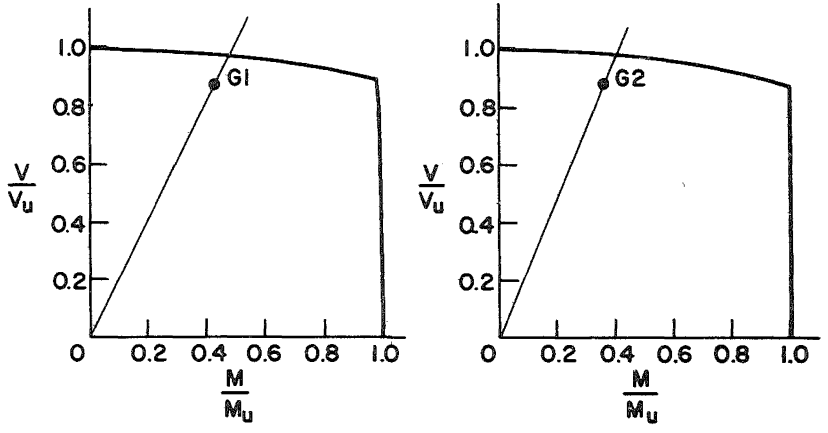

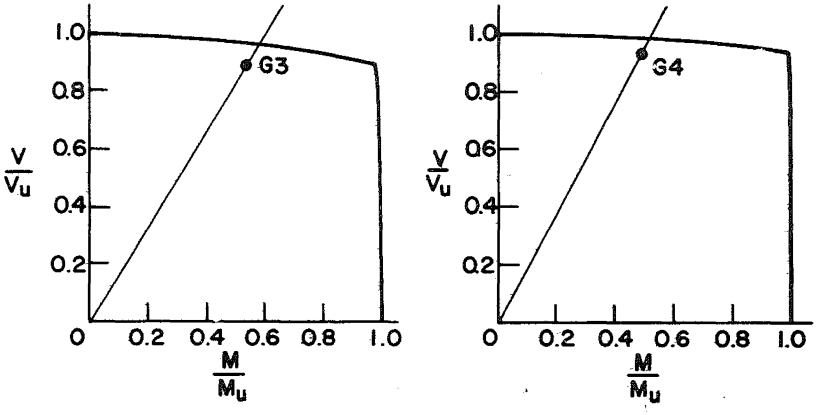

Fig. 14 Interaction Curves and Test Results - G1 to G4 (Ref. 1)

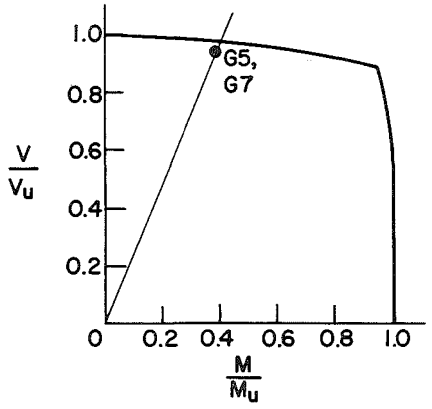

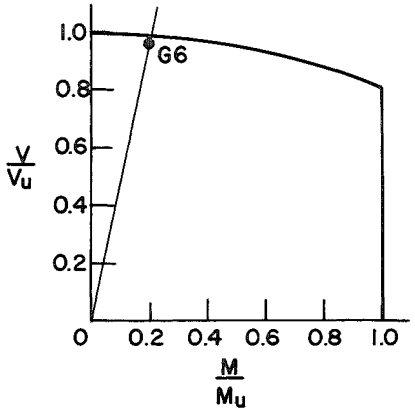

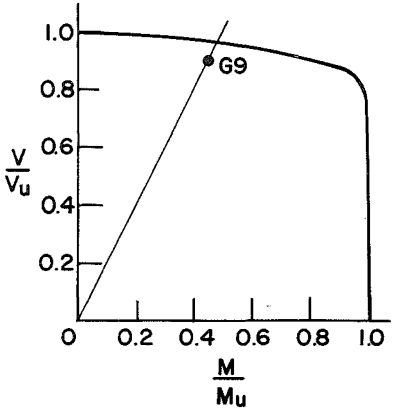

Fig. 15 Interaction Curves and Test Results - G5 to G9 (Ref. 1)

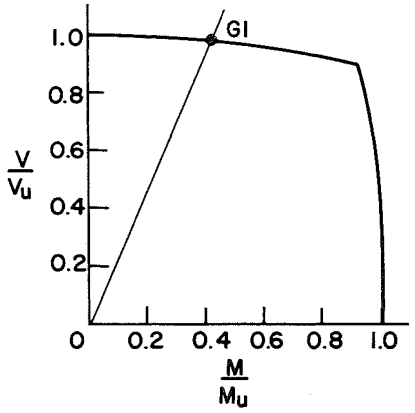

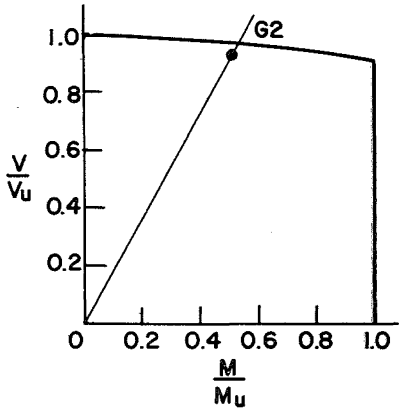

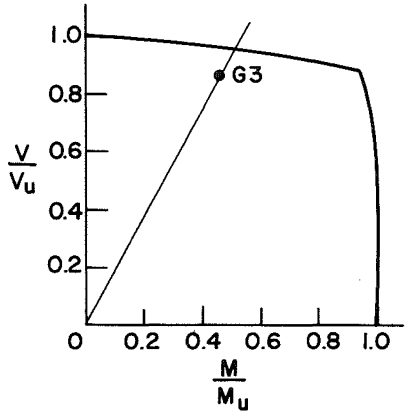

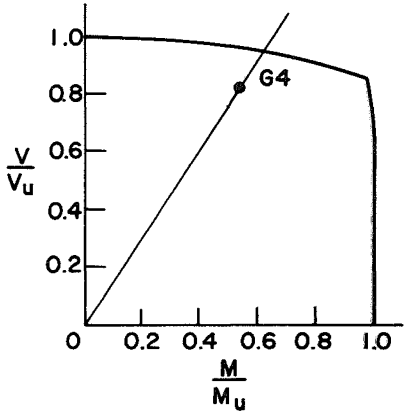

Fig. 16 Interaction Curves and Test Results - G1 to G4 series (Ref. 18)

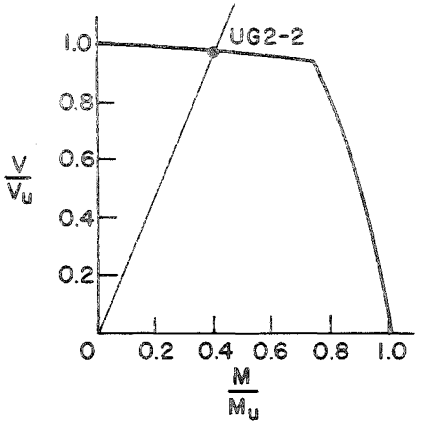

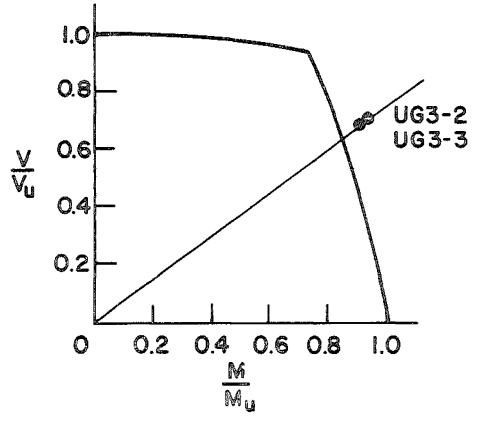

Fig. 17 Interaction Curves and Test Results - UG2 and UG3 Series (Ref. 12)

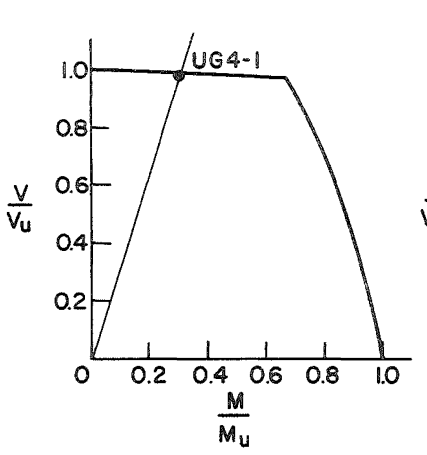

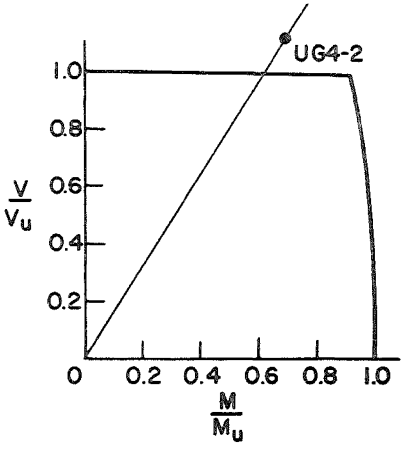

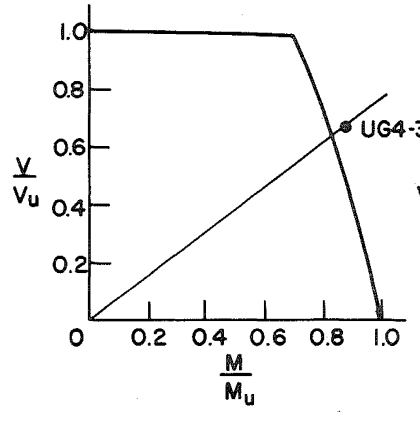

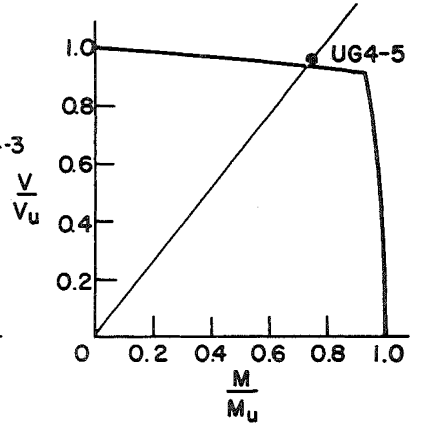

Fig. 18 Interaction Curves and Test Results - UG4 Series (Ref. 23)

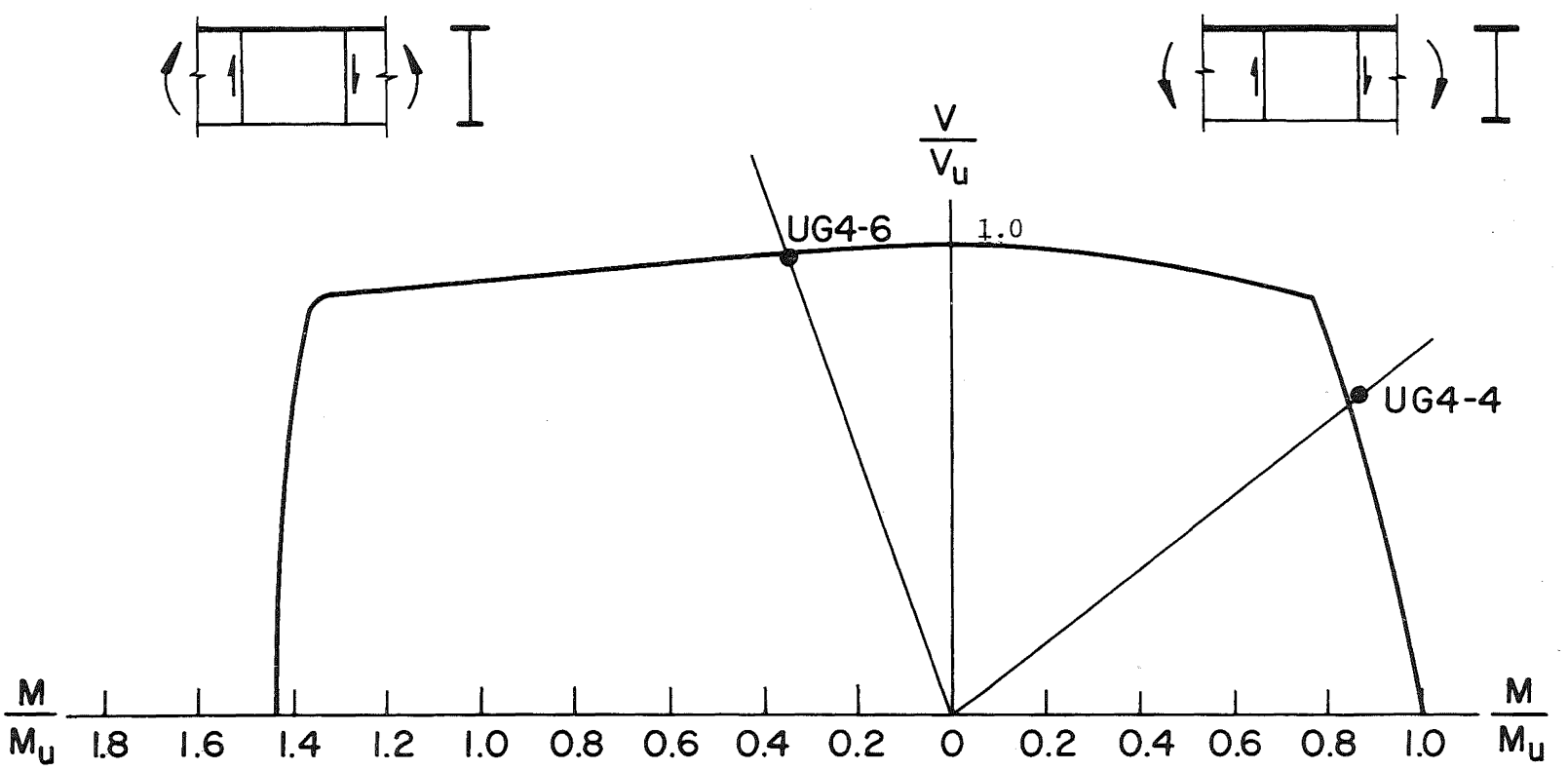

Fig. 19 Complete Interaction Curve and Test Results - UG4.4 and UG4.6 (Ref. 23)

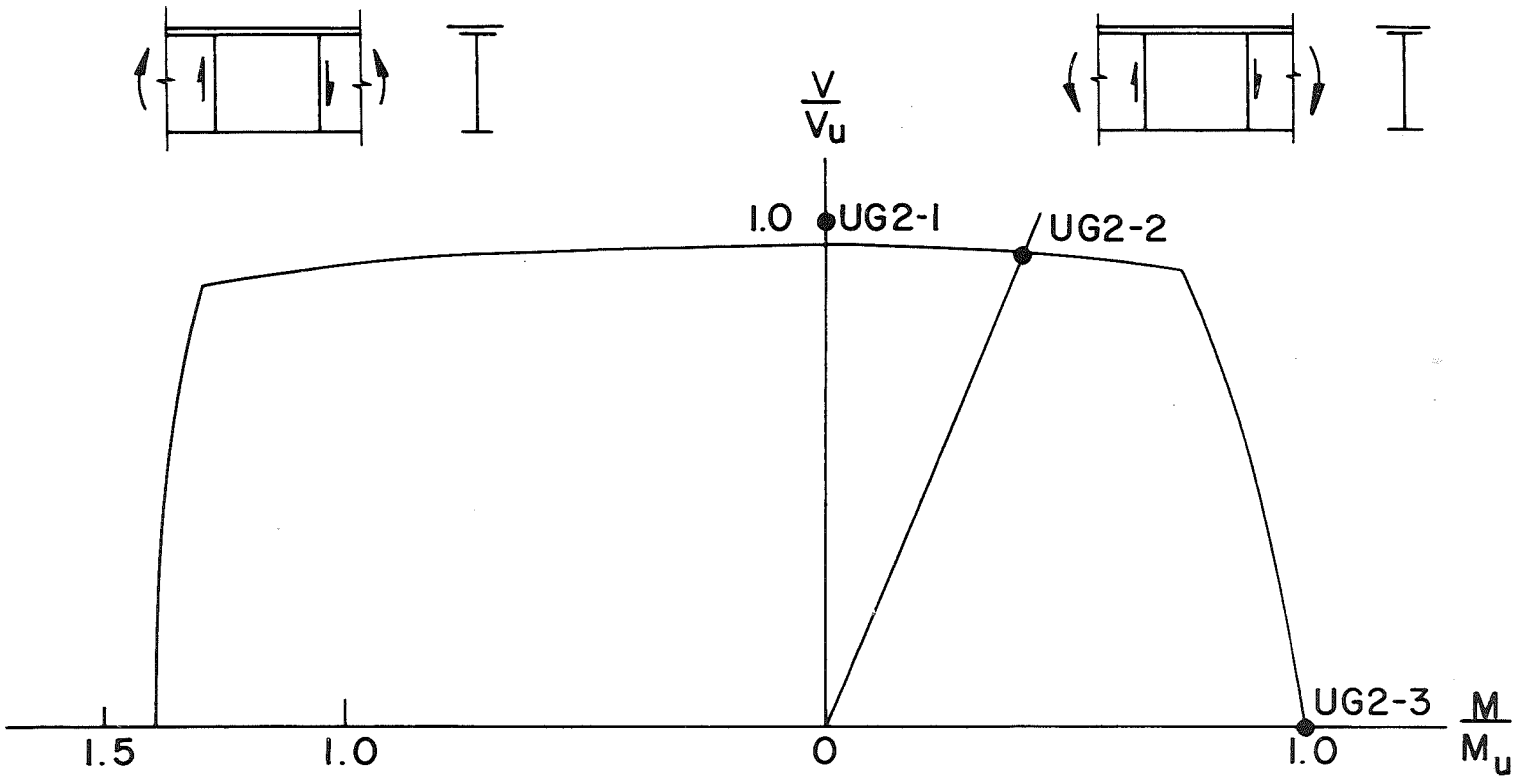

Fig. 20 Complete Interaction Curve and Test Results - UG2 Series (Ref. 12)

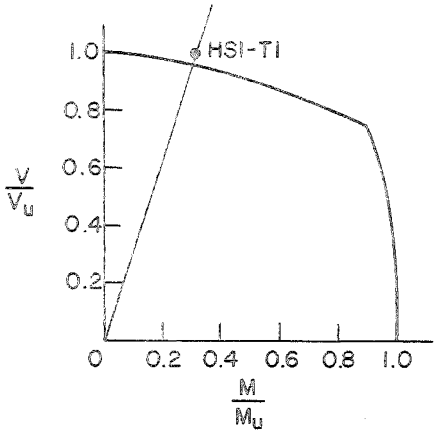

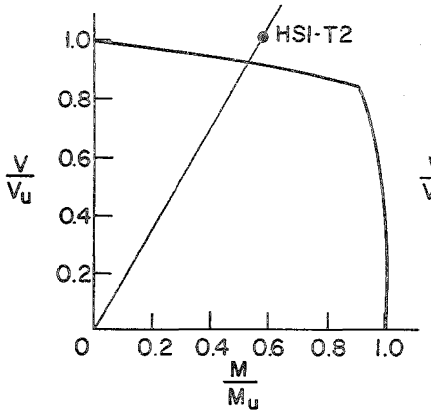

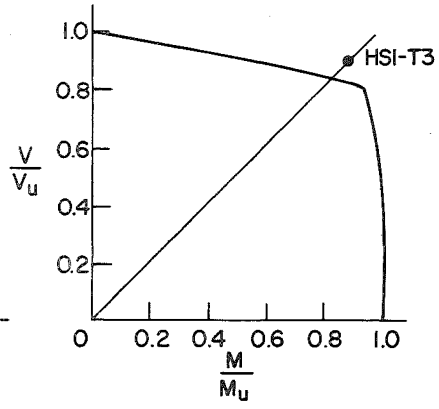

Fig. 21 Interaction Curves and Test Results - HS1 Series (Ref. 16)

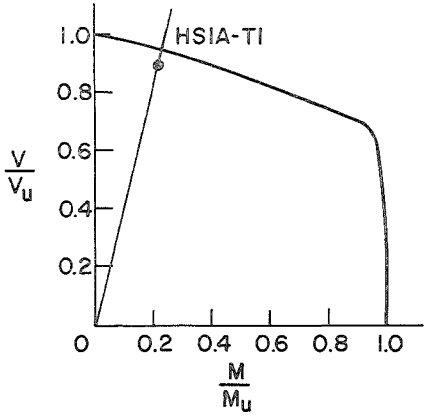

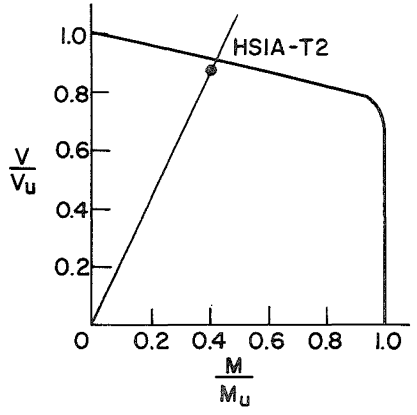

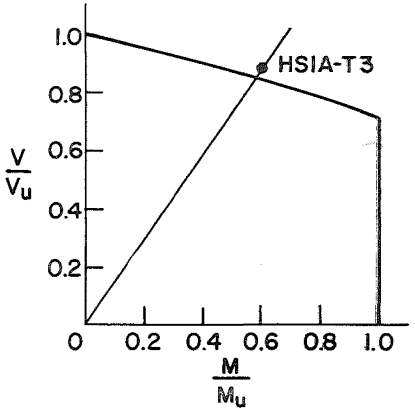

Fig. 22 Interaction Curves and Test Results - HS1A Series (Ref. 16)

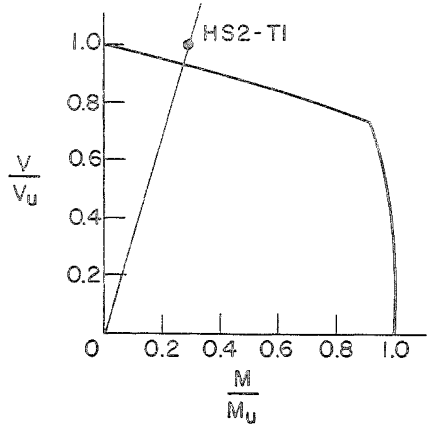

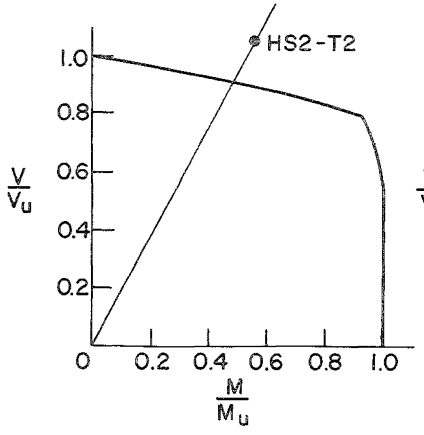

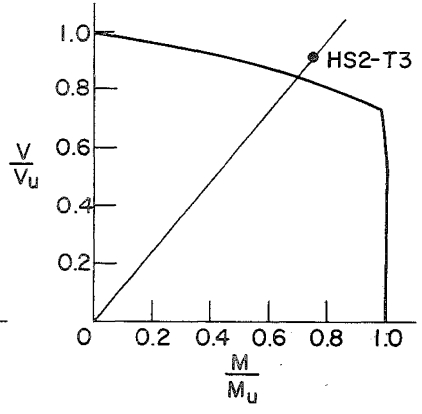

Fig. 23 Interaction Curves and Test Results - HS2 Series (Ref. 16)

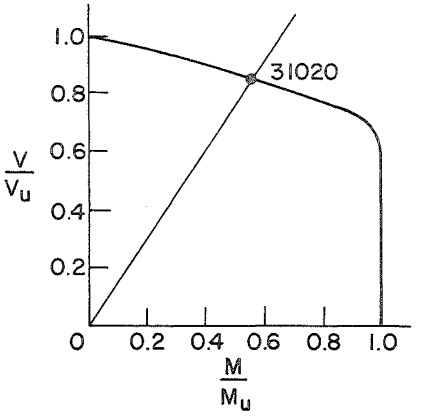

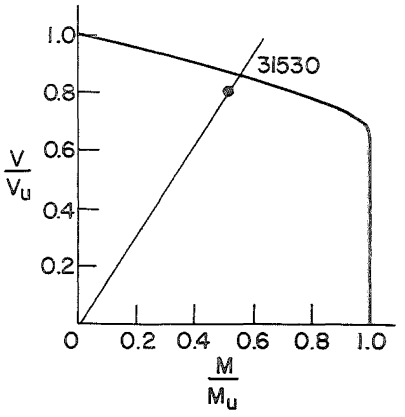

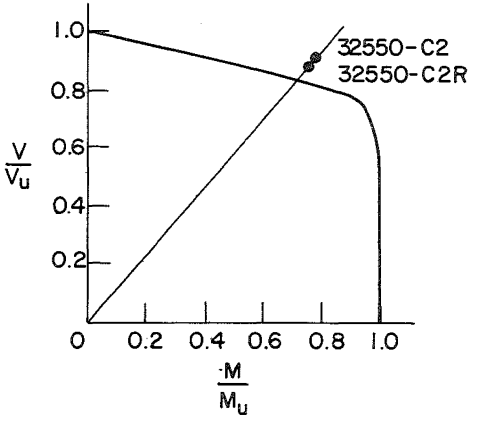

Fig. 24 Interaction Curves and Test Results - (Refs. 13 and 16)

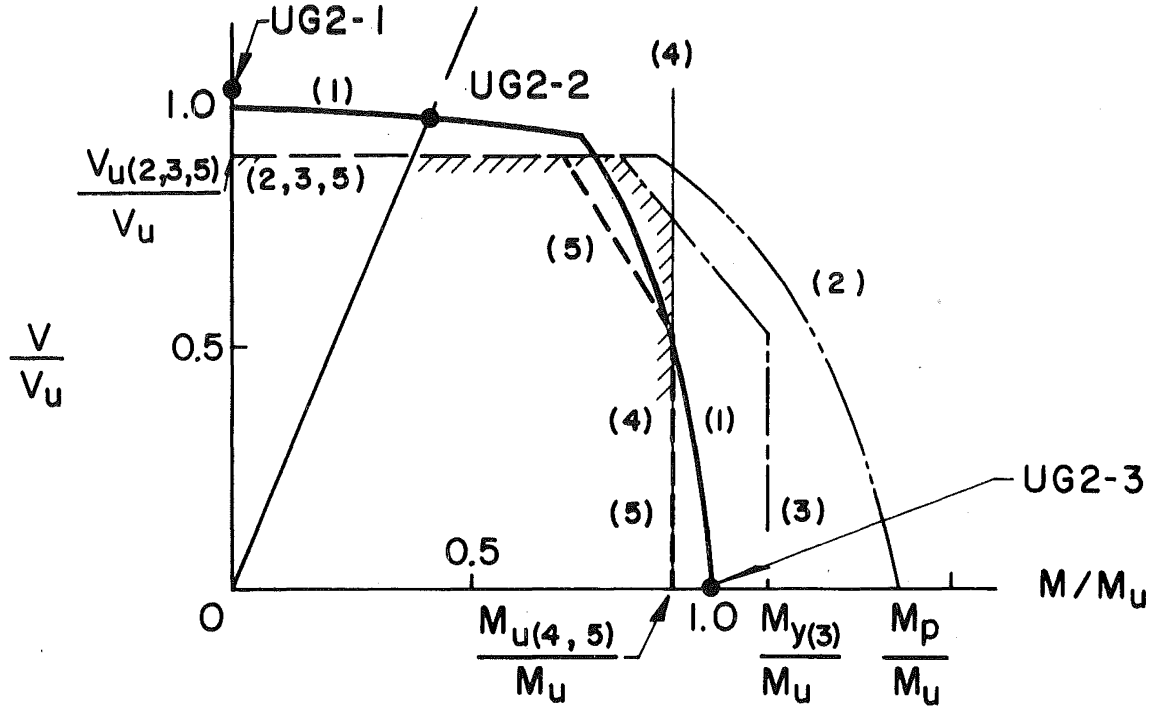

Fig. 25 Comparison of UG2 Series with Various Theories